

Seismogenic slump folds formed by gravity-driven tectonics down a negligible subaqueous slope

G. Ian Alsop ^{a,*}, Shmuel Marco ^b

^a Department of Geology and Petroleum Geology, School of Geosciences, University of Aberdeen, United Kingdom

^b Department of Geophysics and Planetary Sciences, Tel Aviv University, Tel Aviv, 69978, Israel

ARTICLE INFO

Article history:

Received 23 October 2012

Received in revised form 29 March 2013

Accepted 1 April 2013

Available online 10 April 2013

Keywords:

Slope failure

Slump fold

Sheath fold

Soft sediment deformation

MTC

Dead Sea

ABSTRACT

The Late Pleistocene Lisan Formation contains superb examples of soft-sediment deformation generated during gravity-driven slumping and failure down extremely gentle ($<1^\circ$) slopes towards the palaeo-Dead Sea Basin. Following a previously established framework, portions of individual slumps are broadly categorised into coherent, semi-coherent, and incoherent domains, reflecting increasing deformation and disarticulation of sediment. We present new structural data collected from each of these (overlapping) domains that demonstrate how the orientation of fold hinges and axial planes becomes more dispersed as slumps become increasingly incoherent. Such patterns are the reverse to that typically encountered in lithified rocks where increasing deformation results in clustering of linear elements towards the flow direction, and may reflect greater heterogeneity and disarticulation within slumps. Use of folds to determine palaeoslopes should therefore be limited to those from coherent slumps, where the opportunity for hinge dislocation and rotation is more limited. Within coherent and semi-coherent slumps, folds are reworked to create classic Type 1, 2 and 3 re-fold patterns during a single progressive deformation perhaps lasting just a matter of minutes. It is noteworthy that slump folds are typically lacking in smaller parasitic folds, implying that instantaneous development and/or limited viscosity contrasts have hindered the formation of second order folds. As deformation intensifies within semi-coherent to incoherent slumps, some fold hinges rotate towards the flow direction to create sheath folds. However, many fold hinges do not rotate into the flow direction, but rather roll down-slope to form a new category of *spiral folds*. Extreme deformation may also generate semi-detached fold trains in which the short limbs of verging fold pairs are relatively thickened resulting in en-echelon *X folds*. The hinges of the sheared fold pair are reduced to apophyses, although these can still be used to infer original fold vergence. As observations are from a thin slumped system over a relatively small area, the variation in structural style from coherent to incoherent is attributed to increasing deformation.

© 2013 Elsevier B.V. All rights reserved.

1. Introduction

Most text books concerning structural geology and sedimentary processes to some degree neglect structures generated during gravity-driven soft sediment deformation, which occurs prior to the complete lithification of sediments (see Maltman, 1984). This may reflect the fact that this topic spans structural geology, sedimentary systems, and surficial processes associated with slope failure, and perhaps therefore does not fit neatly into any of these categories. In addition, structures generated in soft-sediments will become increasingly difficult to recognise as these become lithified, and possibly undergo subsequent phases of tectonism as hard rocks (see for example, Debacker et al., 2006; Ortner, 2007; Waldron and Gagnon, 2011). Despite these complications, the study of deformation in sediments is growing in importance as the resulting structures affect porosity and permeability of the lithified rock, with obvious implications for fluid flow associated with hydrocarbons and

aquifers (e.g., Hurst et al., 2011). In addition, the study of structures within slump sheets is also important as large-scale systems of gravity-driven deformation associated with slope failure are increasingly recognised on high resolution seismic surveys of continental margins where Mass Transport Complexes (MTCs) are imaged (e.g., Bull et al., 2009; Butler and Paton, 2010; Gardner et al., 1999; Jackson, 2011; Lee et al., 2007). The direct analysis of smaller scale structures at outcrop will therefore help with interpretation of these features, which not only are important in hydrocarbon exploration, but also present significant hazards where modern slope failures can threaten hydrocarbon infrastructure and pipelines (e.g., Locat and Lee, 2002; Mason et al., 2006).

Although failures in modern subaqueous settings can occur on exceptionally low angle slopes of as little as 0.25° (e.g., Field et al., 1982), evidence from the older geological record is frequently interpreted to suggest that more significant slopes are necessary (e.g., Allen, 1982; Lewis, 1971; see Garcia-Tortosa et al., 2011). Detailed studies of modern or relatively recent subaqueous slope failures, which are now exposed at outcrop, can therefore provide further detailed information on the controls and geometries associated with gravity-driven slump systems.

* Corresponding author. Tel.: +44 1224 273438.

E-mail address: Ian.Alsop@abdn.ac.uk (G.I. Alsop).

Finally, the investigation of gravity-driven slump folds and systems is important as it provides wider ranging benefits relating to the analysis of structures (and in particular folds) in other settings where an understanding of flow is important such as salt glaciers (e.g., Aftabi et al., 2010), sub-glacial shear zones (e.g., Lesemann et al., 2010), snow slides (e.g., Lajoie, 1972) and metamorphic shear zones (e.g., see review and references in Druguet et al., 2009).

Deformation within non-cohesive or poorly lithified soft-sediments is largely achieved via independent particulate flow (Knipe, 1986). Relationships between the ratio of pore fluid pressure and cohesive strength of the sediment (due to grain weight) determine the exact nature of the structures that form in the sediment (Knipe, 1986; Ortner, 2007). When fluid pressure is lower than grain weight then hydroplastic deformation develops, leading to primary sedimentary features such as bedding being modified via folds and shears that resemble ductile structures in metamorphic rocks. When fluid pressure is equal to grain weight then sediment liquefies to form laminar flow, in which primary sedimentary features such as bedding are destroyed. When fluid pressure is greater than grain weight then sediment fluidizes to form turbulent flow, in which primary sedimentary features including bedding are destroyed. Increases in pore fluid pressure are achieved by high permeability fluid-rich sediments being overlain by low permeability sediments that act as a seal to prevent fluid escape. Increases in fluid pressure are also temporarily triggered by seismic activity that may ultimately result in fluid pressure exceeding the tensile strength of the surrounding sediment, leading to sedimentary dykes catastrophically injecting into areas of lower pressure and intruding the overlying sequence.

Many studies have examined folds and faults formed during hydroplastic deformation of soft-sediment from the stand-point of guidelines established in the geometric analysis of metamorphic rocks over many decades (Fossen, 2010; Ramsay, 1967; Ramsay and Huber, 1987; Turner and Weiss, 1963). Whilst these undoubtedly provide a valuable framework, an analysis of soft sediment deformation in modern settings, where the gravity-driven component of deformation and direction of slope failure are unambiguous, also presents an opportunity to re-evaluate (and challenge) some of these assumptions. Our study therefore aims to explore and address a number of factors and fundamental questions pertaining to slump folding associated with slope failure including:

- i) How can gravity-driven slumping occur down exceptionally gentle ($<1^\circ$) slopes?
- ii) How do classical re-fold patterns form almost instantaneously within slumps?
- iii) Why do some fold hinges rotate and others roll during slumping?
- iv) What structural patterns are defined by overall slump fold hinges and axial planes as deformation intensifies?
- v) Why do axial surfaces in some slump folds define en-echelon patterns as they step across weaker units?
- vi) Why do small-scale parasitic folds rarely develop around slump folds?
- vii) How representative and useful are structures formed in recent slumps when interpreting those preserved in the geological record?

The purpose of this paper is therefore to address the fundamental questions noted above. We stress however that we are by no means the first to consider some of the basic issues such as how slumping occurs on very low angle slopes (see for example the earlier work of Field et al., 1982; Garcia-Tortosa et al., 2011) and how structures evolve as deformation intensifies within slumps (e.g., Woodcock, 1976a,b, 1979). The Late Pleistocene Lisan Formation exposed on the western shore of the Dead Sea does however provide superb examples of soft sediment deformation associated with slope failure, and this unique opportunity permits perhaps unrivalled excavation and 3-D examination of the resulting slump geometries.

2. Soft sediment deformation

2.1. A theoretical framework for the description of kinematics in slumps

Gravity-driven slumps related to slope failure have been hypothetically modelled as flow cells marked by extension in the upslope regime that is broadly balanced by contraction in the lower downslope or toe area of the slump (e.g., Collinson, 1994; Elliot and Williams, 1988; Farrell, 1984; Farrell and Eaton, 1987; Hansen, 1971; Lewis, 1971; Martinsen, 1989, 1994; Martinsen and Bakken, 1990; Smith, 2000; Strachan, 2002, 2008). Slope failure is considered to initiate at a single point and generates a compressive wave that spreads downslope and an extensional wave that propagates upslope (Farrell, 1984) (Fig. 1a). Subsequent translation of the slumped mass results in compressional folds and thrusts at the downslope toe of the system, whilst the head is marked by extensional

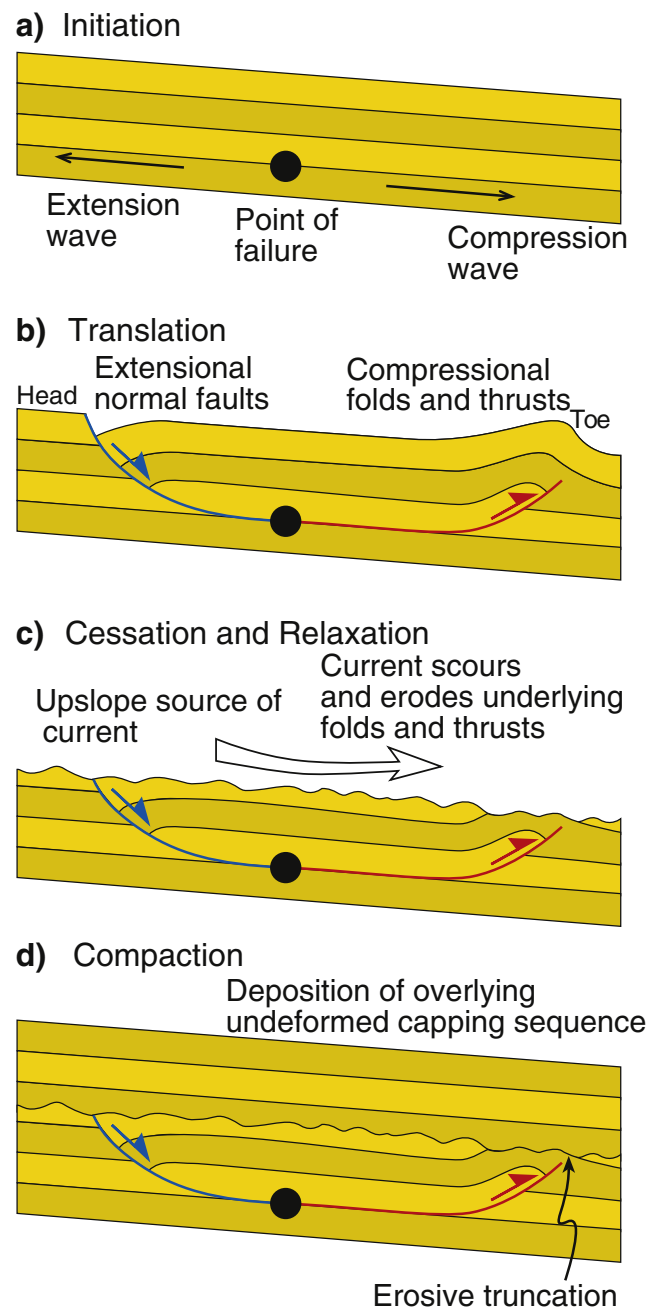


Fig. 1. Schematic cartoons illustrating the initiation (a), translation (b), cessation and relaxation (c), and subsequent compaction (d) of a hypothetical slump sheet.

normal faults (Fig. 1b). As extensional faults develop during cessation of movement they may (repeatedly) cut the sediment surface and create further slope failure associated with turbidity flows (Fig. 1c). Such currents travel downslope where they scour and erode surficial features associated with compressive folds and thrusts created during the same event. Alternatively, scouring can be generated in relatively shallow water settings by the action of tsunami and seiche waves that flow back and forth across the slumped surface (Alsop and Marco, 2012b). In both scenarios, folds and faults are finally capped by deposition of overlying sediments resulting in compaction and flattening of slump geometries (Fig. 1d).

The flow cell model outlined above provides a theoretical kinematic framework for the analysis of folds and faults associated with slope failure. Slump fold hinges are classically considered to initiate at the downslope toe of the failure surface, form parallel to the strike of the slope (e.g., Jones, 1939), and verge downslope such that axial planes will dip in the upslope direction (e.g., Woodcock, 1979). This simple pattern will become more complicated if such fold hinges subsequently rotate towards the downslope direction during continued movement, resulting in a wide range of hinge orientations and potential curvilinear or sheath fold geometries in extreme cases (e.g., Alsop and Holdsworth, 2012; Strachan and Alsop, 2006). Whilst fold hinges rotate into the downslope flow direction, associated axial planes rotate towards the shear plane resulting in a reduction in fold interlimb angles (e.g., Alsop and Marco, 2011, 2012a,b; Woodcock, 1979).

The classic fold patterns described above are generated where deformation is dominated by layer-parallel shear (LPS) along an underlying detachment marking the failure surface, such that displacement is broadly equal along the strike of the slope (see Alsop and Marco, 2011, 2012a,b). However, where displacement along the failure surface is variable along the strike of the slope, then differential movement marked by layer-normal shear (LNS) will develop (Alsop and Holdsworth, 2007). This adds significant complexity as fold hinges will initiate at variable angles to the slope direction, and the simple relationship between fold orientation and slope direction therefore breaks down (see Alsop and Marco, 2012a; Debacker et al., 2009; Strachan and Alsop, 2006). Similar complexities have been recognised in other settings that undergo progressive non-coaxial dominated deformation such as periglacial slope failures (e.g., Hansen, 1971), snow slides (e.g., Lajoie, 1972), salt glaciers (e.g., Aftabi et al., 2010), below ice sheets (e.g., see Lesemann et al., 2010) and within metamorphic shear zones (e.g., Druguet et al., 2009).

2.2. A framework for the description of facing in slumps

As well as the asymmetry or vergence of folds that marks the sense of overturning of the fold short limb, it is also possible to calculate the direction of fold facing. Following the original work of Shackleton (1958), fold facing is here defined as the direction, normal to the fold hinge and along the axial plane, in which younger rocks are encountered (see Holdsworth, 1988; Strachan and Alsop, 2006). Facing is therefore a directional measurement with an upward or downward component that plots as a point on a stereonet. The facing direction in slump folds is upwards and parallel to the direction of the slope in situations where fold hinges form broadly parallel to the strike of the slope and undergo little or no subsequent rotation (Alsop and Marco, 2011, 2012a,b; Woodcock, 1976a,b). However, where fold hinges have suffered later rotation during progressive shearing to create curvilinear sheath fold geometries, then facing attitudes will typically become sub-horizontal and define a range of directions reflecting the arc of hinge orientations (e.g., Alsop and Holdsworth, 2007; Strachan and Alsop, 2006). As noted previously, differential shear (LNS) within slumped masses will also encourage folds to initiate (and hence face) at a range of angles to the slope direction.

2.3. A geometric framework for the description of deformation in slumps

For the purposes of general comparison of slump-related folds, observations of fold geometries are broadly classified into coherent, semi-coherent and incoherent styles associated with increasing deformation within the slump (following for example Corbett, 1973; Dzulynski and Walton, 1965, p.191; Pickering, 1987). Coherent is defined as “consistent, connected and orderly” (Chambers Dictionary, 1993) and bedding can be traced with confidence around well-defined, cm–m scale folds formed during weak–moderate deformation within coherent portions of slumps. Semi-coherent is defined as partially or almost consistent and orderly, and bedding becomes increasingly disrupted by discontinuities associated with thrusts and detachments within the strongly deformed semi-coherent portions of slumps. Incoherent is defined as “lacking in clarity or organisation” (Collins English Dictionary & Thesaurus, 2000) and the bedding has become disarticulated, whilst folding is largely detached and isolated within the matrix of the intensely deformed incoherent portions of slumps.

Thus, coherent portions of slumps are defined as where bedding can be traced continuously, including around folds, whereas semi-coherent portions of slumps are defined as where fold limbs are attenuated and even excised. Incoherent portions of slumps are defined by the disaggregation of folds that have become detached in the surrounding matrix. Clearly there may be a degree of overlap between structures formed in these groupings, but this non-generic classification does form a useful framework to describe folds created during a single slump event. It should however be noted that the style of deformation within slump horizons can vary laterally from over a few metres (e.g., Pickering, 1987) and that a continuum of structures may be developed during progressive deformation within slump sheets (e.g., Alsop and Marco, 2011). We now provide an outline of the regional geology around the Dead Sea Basin, before presenting new data and detailed observations of fold and fabric geometries from the slump system that forms our case study.

3. Geological setting of the Dead Sea case study

The Dead Sea Basin is an ideal place to study sediment deformation associated with slope failure as it is a pronounced but relatively simple basin, where subtle slopes controlling gravity-driven slump complexes are exceptionally well preserved. The Dead Sea Basin is a pull-apart structure on the Dead Sea transform, which is marked by two parallel fault strands (Garfunkel, 1981; Garfunkel and Ben-Avraham, 1996) that generate numerous earthquakes with which to trigger slope failure and slumping (see below) (e.g., Begin et al., 2005; Ken-Tor et al., 2001; Marco et al., 1996, 2003; Migowski et al., 2004) (Fig. 2a, b). The transform is considered to have been active since the Miocene, including during deposition of the Lisan Formation in the Late Pleistocene (70–15 ka) (e.g., Bartov et al., 1980; Garfunkel, 1981; Haase-Schramm et al., 2004).

The rates of tectonic deformation in the Dead Sea Basin, where the Lisan Formation outcrops, are of the order of 5 mm/yr of left lateral plate motion. However, the vertical component is significantly smaller with the long-term subsidence estimated at 0.5–0.6 mm/yr based on a refraction survey that shows 8 km of basin fill (Ginzburg and Ben-Avraham, 1997) during the last 15 million years (Garfunkel and Ben-Avraham, 1996). Sedimentation rates in the Late Quaternary are of the order of just 0.8–0.9 mm/yr. Thus, the rates of vertical motion and subsidence are therefore too small to cause a significant tilt of the Lisan Formation, and the observed regional dip of <1° towards the east represents the original subtle depositional dip towards the basin (see Alsop and Marco, 2012a).

Three key observations have led previous workers to the conclusion that earthquakes have triggered slumps within the Lisan Formation: First, slump and breccia layers are directly associated with slip on syn-depositional faults within the Lisan Formation (Marco and Agnon,

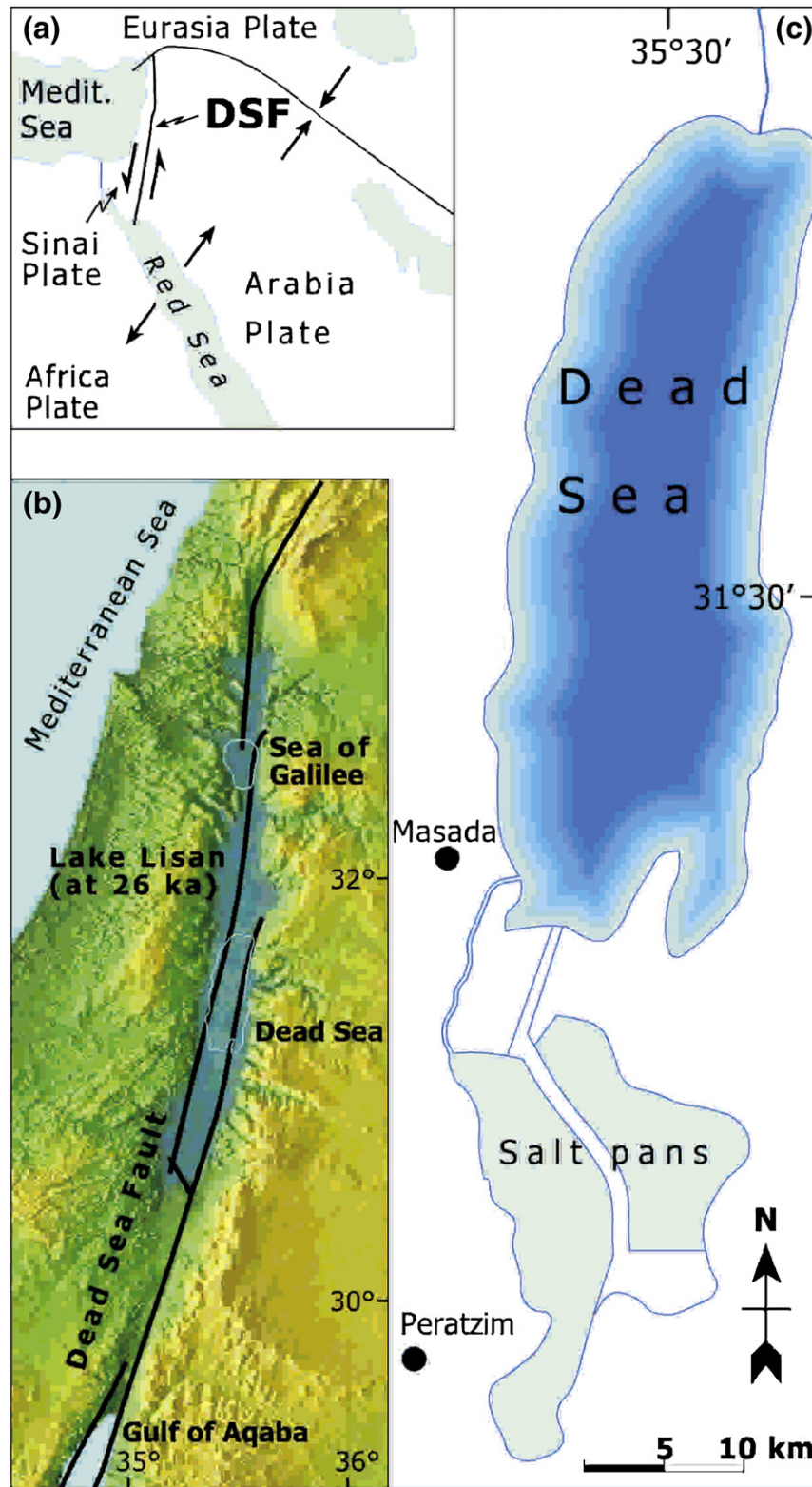


Fig. 2. Introductory map of the Dead Sea and localities referred to in the text a) tectonic plates in the Middle East. General tectonic map showing the location of the present Dead Sea Fault (DSF). The Dead Sea Fault transfers the opening motion in the Red Sea to the Taurus–Zagros collision zone. b) Generalised map showing the maximum extent of Lake Lisan along the Dead Sea Fault at 26 ka. c) Map of the current Dead Sea showing the position of localities and the case study area of Peratzim.

1995, 2005). Second, the slump horizons appear to be gravitationally stable as a) they are associated with relatively slow rates of deposition in the Lisan Formation (see above), and b) are underlain by nearly horizontal detachment planes, hence, the slumping requires a trigger

(Alsop and Marco, 2011). Third, ages of similar slump structures in the Late Holocene Ze'elim Formation coincide with historical earthquakes (Kagan et al., 2011; Ken-Tor et al., 2001; Migowski et al., 2004). The case study area within the Lisan Formation therefore provides

a superb opportunity to study the nature and geometry of seismogenic slump folds.

The Lisan Formation comprises a sequence of finely laminated aragonite-rich and clastic-rich couplets considered to represent annual varve-like cycles (Fig. 3a, b). Aragonite-rich laminae precipitate from the hypersaline water during dry summers, whilst clastic-rich layers are considered to be washed into the basin during winter storm events (Begin et al., 1974; Migowski et al., 2004). Slumping within the Lisan Formation is thought to have been triggered by seismic activity along the Dead Sea transform, with the very subtle depositional dips of $<1^\circ$ noted above controlling the direction of radial slumping toward the Dead Sea Basin (e.g., see Alsop and Marco, 2012b). Slumped units are exceptionally well preserved, are typically less than 1.5 m thick, and are capped by undeformed sediment of the overlying Lisan Formation (Alsop and Marco, 2011). In addition, the slumped units are cut by

sedimentary injection dykes containing fluidised clastic material sourced from underlying units (e.g., Levi et al., 2006; Marco et al., 2002). The optically stimulated luminescence (OSL) ages of quartz grains were reset from between 43 and 34 ka to between 15 and 17 ka within the sedimentary dykes, indicating that they intruded after deposition of the Lisan Formation (Porat et al., 2007). Although late-stage fluidisation clearly occurred to generate the cross-cutting sedimentary dykes, the deformation within the slumped unit is considered to be hydroplastic as bedding can be traced around the resulting folds (see Section 4.). The cross cutting sedimentary dyke relationships do however categorically demonstrate that folds and faults were formed prior to complete lithification of the sequence.

The Lisan Formation is ideal for the detailed study of slump folds and faults as a) it is marked by an intricate varved stratigraphy on a mm-scale permitting even the slightest deformation to be recorded;

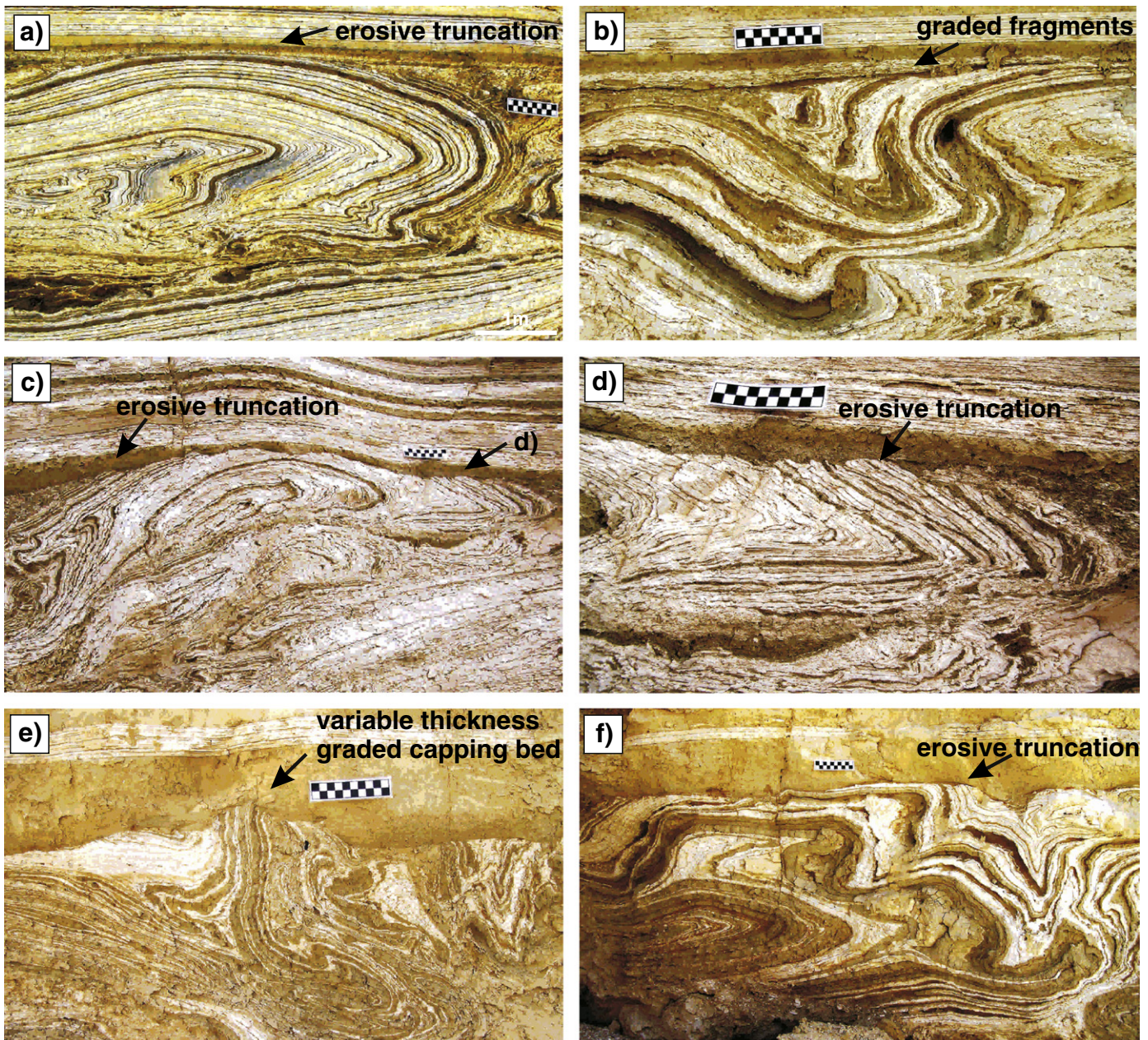


Fig. 3. Representative photographs of slump folds at Peratzim being truncated by overlying erosive surfaces. In a) and b), the erosive surface is capped by a thin (2–3 cm) clastic horizon that displays normal grading of light-coloured aragonite fragments. The thickness of this capping bed is observed to vary laterally in c) as the upper limb of an underlying recumbent slump fold is truncated. Details of the erosive truncation on the right hand side of c) are shown in d). The graded capping horizon is up to 20 cm thick in e) and f) and displays pronounced thickness variations to infill the underlying truncated slump folds. All photos are orientated with NE towards the right and have a chequered 10 cm rule for scale.

b) the stratigraphy is layer-cake meaning that original sedimentary thickness variations on the scale of the exposure can be discounted when examining detailed structural geometries; c) dark clastic and white aragonite-rich couplets alternating on a mm-scale provide an almost perfect bar-code template allowing sequences to be correlated with confidence around folds and across faults (Fig. 3a, b) (Alsop and Marco, 2011); d) slumped horizons are clearly bound both above and below by undeformed sequences providing a stratigraphic reference frame for their analysis (e.g., Bradley and Hanson, 1998); and e) the Lisan Formation remains poorly lithified meaning that, although the preparation of thin sections is not typically possible, its unconsolidated nature does allow easy excavation to reveal 3-D structural geometries. Photographs and illustrations that follow are placed with northeast consistently on the right-hand side and have scales represented by a coin (15 mm diameter), chequered cm rule (10 cm long) and a hammer (30 cm shank with a 15 cm head).

4. General observations of slump fold geometries

We have examined different parts of a slump system that can be confidently traced for 250 m across strike and downslope via a series of wadi exposures at Peratzim in the southern Dead Sea Basin (N31° 0449.6, E35° 2104.2) (see Alsop and Marco, 2011) (Fig. 2c). The slumps are considered to have been exposed at the sediment surface at the time of deformation as a) slump related folds and structures are truncated by an overlying erosive surface that formed due to rapid water flow (Fig. 3a–f) (see Alsop and Marco, 2012b); b) the slumps are typically draped by an overlying clastic horizon that displays upward fining of aragonite fragments interpreted as graded bedding formed when sediment is deposited out of suspension (Fig. 3b); and c) the undeformed beds overlying the slumps are observed to thicken

and thin over slump geometries, indicating that the sediment filled local decimetre-scale slump bathymetry (Fig. 3c–f). The effects of such sediment draping extend for up to 0.5 m into the overlying undeformed sequence (see Alsop and Marco, 2012b for further details).

Thus, the observed folds and structures do not represent overpressure-triggered deformation associated with liquidisation or fluidisation beneath an overburden. Rather, erosive truncation at the top of the slumped layers, together with upward-fining of the aragonite fragments in the overlying clastic unit that drapes and infills bathymetry clearly indicates that the slumped strata formed at the sediment–water interface during hydroplastic deformation were associated with slope failure. The asymmetry of the folds and the homogeneous nature of the sediment indicate that the folding is related to gravity-driven shear rather than inverse density (Heifetz et al., 2005; Wetzler et al., 2009).

The <1.5 m thick slumps are consistently positioned above, and are observed to locally detach on to, 5–10 cm thick mud-rich horizons that acted as weak décollements (Figs. 4a, 5a, c, e). Similar relationships between slumps and underlying mud and clay-rich horizons are observed elsewhere, and are attributed to fluid overpressure significantly weakening the mud and facilitating failure and slumping even on very gentle (<1°) slopes (e.g., Garcia-Tortosa et al., 2011; Strachan, 2002). Fold hinge and axial plane orientations, together with fold style, were examined and recorded at a series of sites broadly classified as representing coherent, semi-coherent and incoherent portions of the slumped system at Peratzim. The fold and fabric data in each setting are then compared with the general trend of structures and inferred orientation of the NE-directed (040°) palaeoslope (see Alsop and Marco, 2012a). As all of these sites are dominated by pronounced folding and thrusting, they are all interpreted to lie in the overall downslope contractional portion or toe of the slump system (see Section 2.1., Alsop and Marco, 2011).

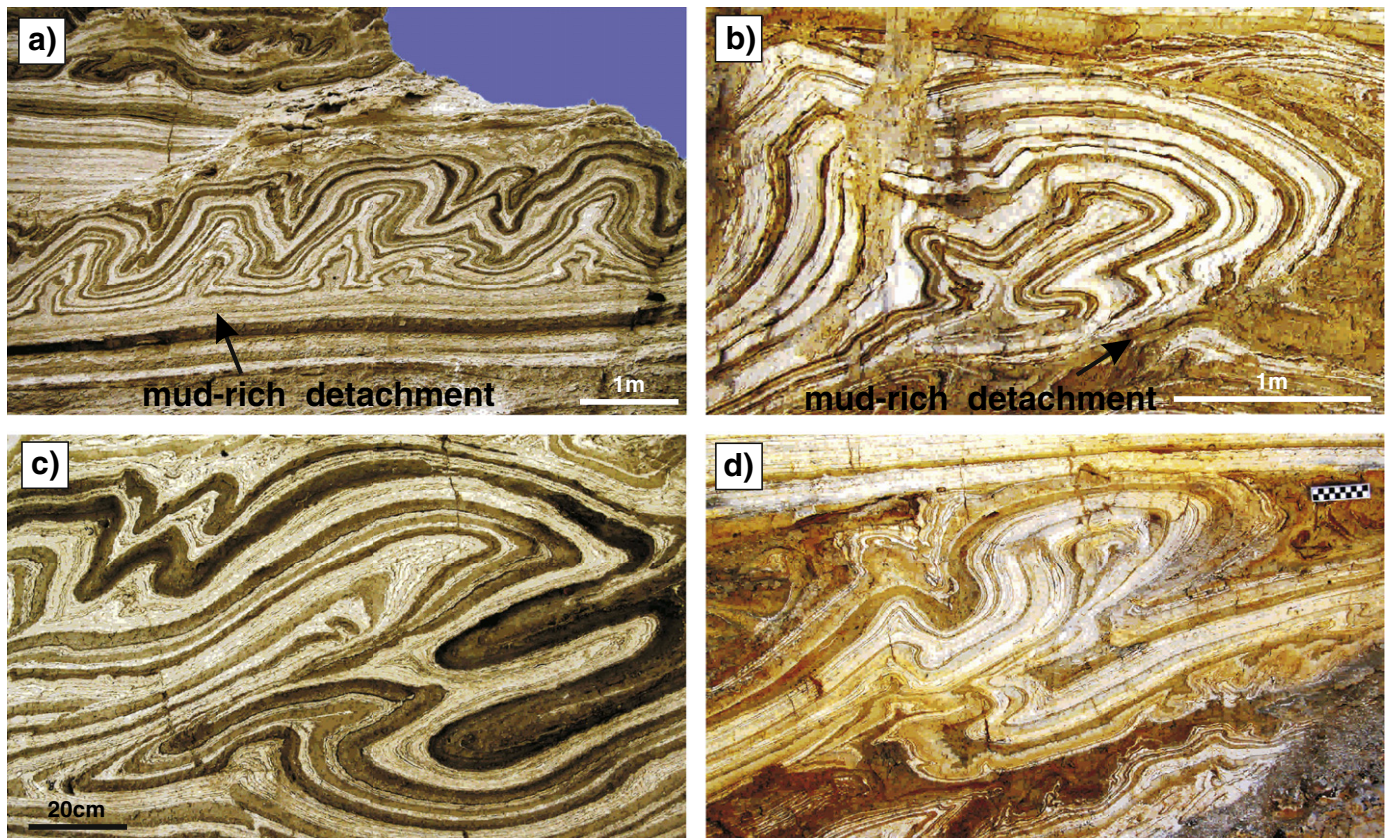


Fig. 4. Representative photographs of folds from coherent (a, b) and semi-coherent (c, d) portions of the slump at Peratzim. Note that bedding can be traced continuously around folds in coherent slumps, whereas the lower fold limbs are frequently attenuated and even excised within semi-coherent slumps. All photos are orientated with NE towards the right and have a coin (15 mm diameter), chequered rule (10 cm long) or hammer (30 cm long) for scale.

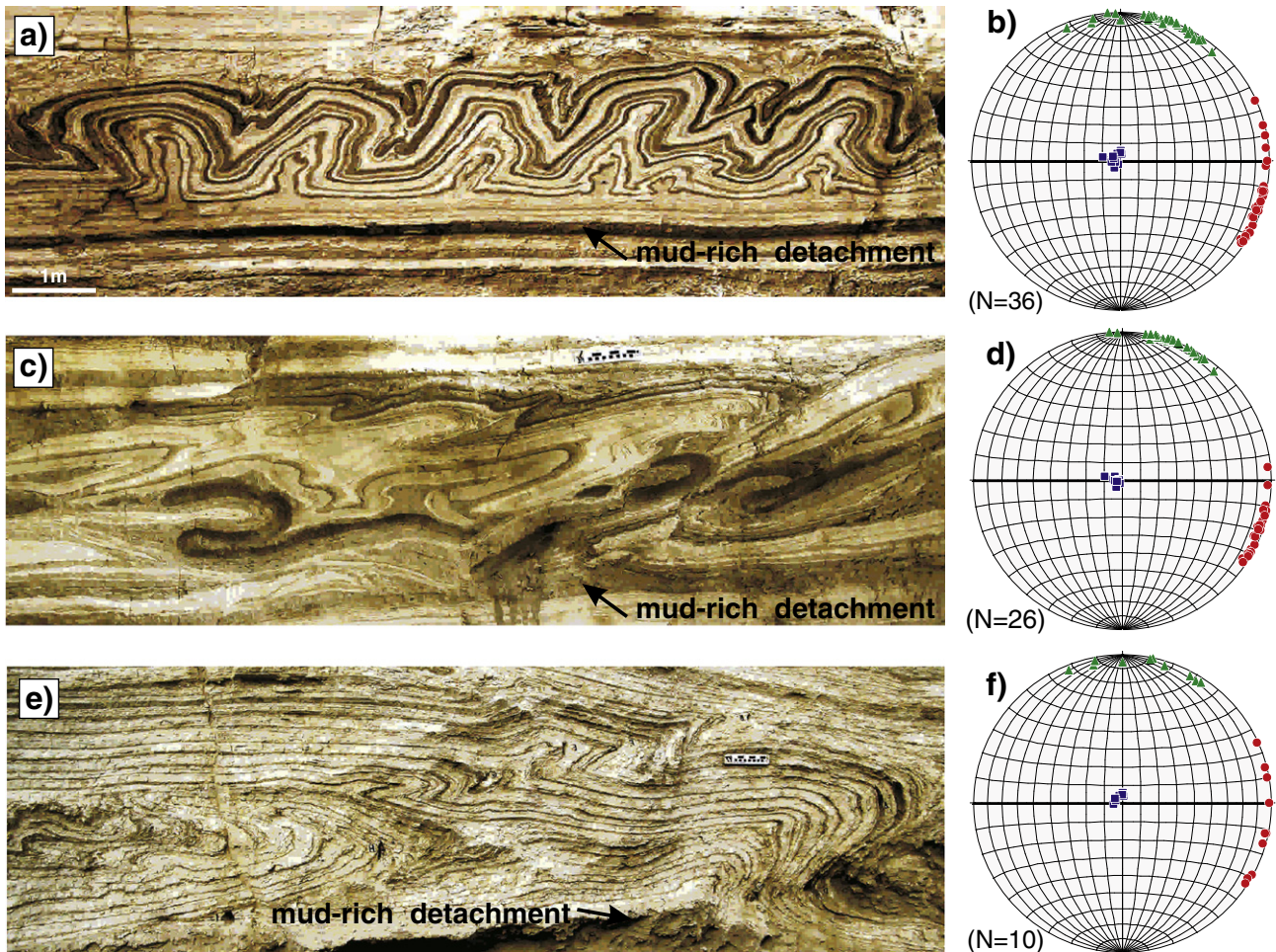


Fig. 5. Sets of representative photographs (a, c, e) and stereonets (b, d, f), from the coherent portions of the case study slump system at Peratzim. Photo (a) and the associated stereonet (b) show overall data from coherent slumps, whilst photos and associated stereonets (c,d) and (e,f) show data from individual structures. The photographs show the NE-verging slump capped by undeformed sub horizontal beds. Equal area stereoplots show fold hinges (solid red circles) and poles to the axial surfaces (blue squares). Upward facing directions are projected vertically down (as chordal points) from their upper hemisphere intersection onto the lower hemisphere stereonet (green triangles).

5. Observations from weakly–moderately deformed coherent portions of slumps

The weakly–moderately deformed portions of slumps are marked by coherent structures, in which the bedding can be traced continuously around cm–m scale folds (see Section 2.3. for definitions). In general there are a large proportion of units comprising intact aragonite-rich laminae within the coherent parts of the slump (Fig. 4a, b). Folds are observed to detach in or just above an underlying mud-rich unit, which is considered to have acted as a weak decollement that facilitates slope failure and slumping (Fig. 5a, c, e).

Fold hinges plunge very gently towards the ESE with associated axial planes dipping very shallowly towards the east (Fig. 5b, d, f), although gentle–moderate west dipping axial planes are also observed. Fold hinges plunge consistently towards the east (mean $2/107^\circ$) with trends distributed over a relatively limited 60° arc (Fig. 5b, d, f). Uniformity of orientation, together with direct observation, indicates that many of these fold hinges are largely cylindrical. There is a pronounced asymmetry to folds with vergence directed consistently towards the NNE (Fig. 5a, c, e). Associated fold facing is also directed towards the N and NNE (Fig. 5b, d, f).

In summary, coherent slumps are well organised with bedding forming clearly defined folds that are consistently orientated normal to the 040° slope direction within the case study. As folds within coherent portions of slumps tend to initiate and remain at high angles

to the slope direction, deformation within the Lisan Formation is considered to be dominated by layer-parallel shear (LPS) (see Alsop and Marco, 2011, 2012a,b). We now describe some of the typical fold geometries developed within the coherent portions of slumps.

5.1. Detachment folds

Detachment folds form where layers above a detachment marking slope failure shorten more than their substrate, which in some cases remains entirely undeformed (e.g., Fossen, 2010 p.322). They tend to form via buckling above weak easy-slip horizons along which the detachment propagates, and can form on any scale. Mud-rich horizons that are up to 10 cm thick can act as detachments within the Lisan Formation. Detachment folds in the case study slump are typically upright, and display box fold geometries with axial planes at each hinge or corner of the box dipping in opposite directions and converging downwards at a single point (Figs. 4a, 5a, 6). The upright box folds root downwards onto the detachment and display a parallel fold style with relatively constant layer thickness (measured normal to bedding) and wavelength indicating a buckle fold mechanism. Woodcock (1979) studied patterns of lineations that are deformed around slump folds and found that they typically indicate a buckle fold mechanism. Within the Lisan Formation, the weak mud-rich layer immediately above the detachment flows to fill the hinges of the fold and accommodate the parallel fold style in the overlying

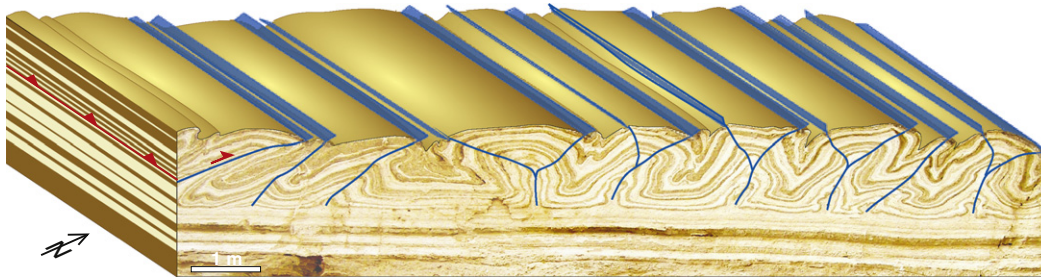


Fig. 6. Photograph and schematic interpretative top surface of a metre-scale fold and thrust system translating downslope towards the NNE at Peratzim. The ~13 m section comprises upright folds that develop above an undeformed sequence. The box folds typically display bifurcating axial planes (highlighted in blue) that root downwards onto an underlying detachment. Downslope vergence towards the NNE becomes more pronounced towards the left-hand side of the image where thrusting is observed.

layers that are completely decoupled from the undeformed substrate (Figs. 5a, 6). Although the detachment fold trains display overall downslope vergence, this is complicated by the upright nature of the folding coupled with bifurcating axial planes (Fig. 6). If distributed simple shear deformation continues to develop, then box folds become overturned with axial planes inclined upslope and thrusts developing on overturned limbs. This permits the downslope direction to be determined with greater confidence (Fig. 6).

5.2. Modification of pre-existing folds

As noted above, simple shear modification of upright symmetrical folds results in the development of increasingly inclined asymmetric folds (Fig. 5c, e). Asymmetric folds are marked by long limbs in the extensional field becoming stretched and thinner, whilst short limbs have rotated into the contractional field and become thicker (Fig. 7a, b). Differences in the ratio of limb lengths (asymmetry) and thicknesses will increase as the axial plane rotates increasingly towards the sub-horizontal shear plane (e.g., Alsop and Carreras, 2007).

Simple shear modification of monoformal folds verging in the direction of shear is marked by sub-horizontal long limbs lying parallel to the

shear plane, and this limb will not therefore undergo rotation and thickness changes (Fig. 7c, d). Conversely, the steeper limb eventually rotates into the extensional field resulting in attenuation and ultimate failure of this short limb (Fig. 7c, d). In summary, a variation in limb thickness around slump folds therefore directly reflects the earlier fold orientation and geometry. Similar patterns are observed around tectonic folds, where a variation in layer thickness has been used to infer vergence in complex curvilinear folds (e.g., Fossen and Rykkeldid, 1990) (see Section 7.2.).

6. Observations from strongly deformed semi-coherent portions of slumps

The strongly deformed portions of slumps are marked by semi-coherent structures in which bedding can be traced around cm–m scale folds but becomes increasingly disrupted by discontinuities on lower fold limbs (Fig. 4c, d). These thrusts and detachments are observed to root downwards into underlying mud-rich units, that may have facilitated deformation on the very gentle (<1°) slopes (Fig. 8a, c). In general there is a greater proportion of disaggregated sediment and mud-rich units within the semi-coherent parts of slumps. Fold hinges plunge

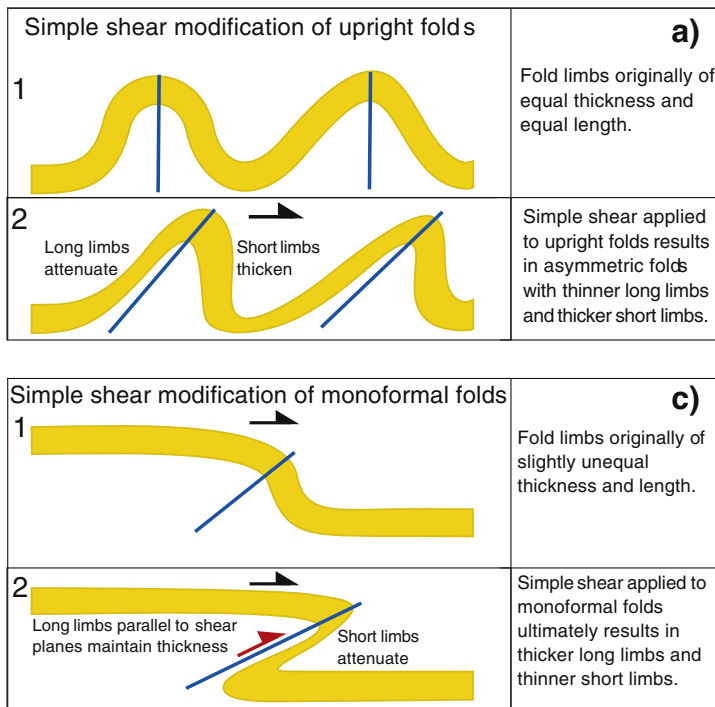


Fig. 7. Schematic sketches of sub horizontal simple shear applied to a) upright folds and an associated field example from Masada (b), and monoformal folds (c) and associated field example from Peratzim (d). Refer to Fig. 2c. for locations.

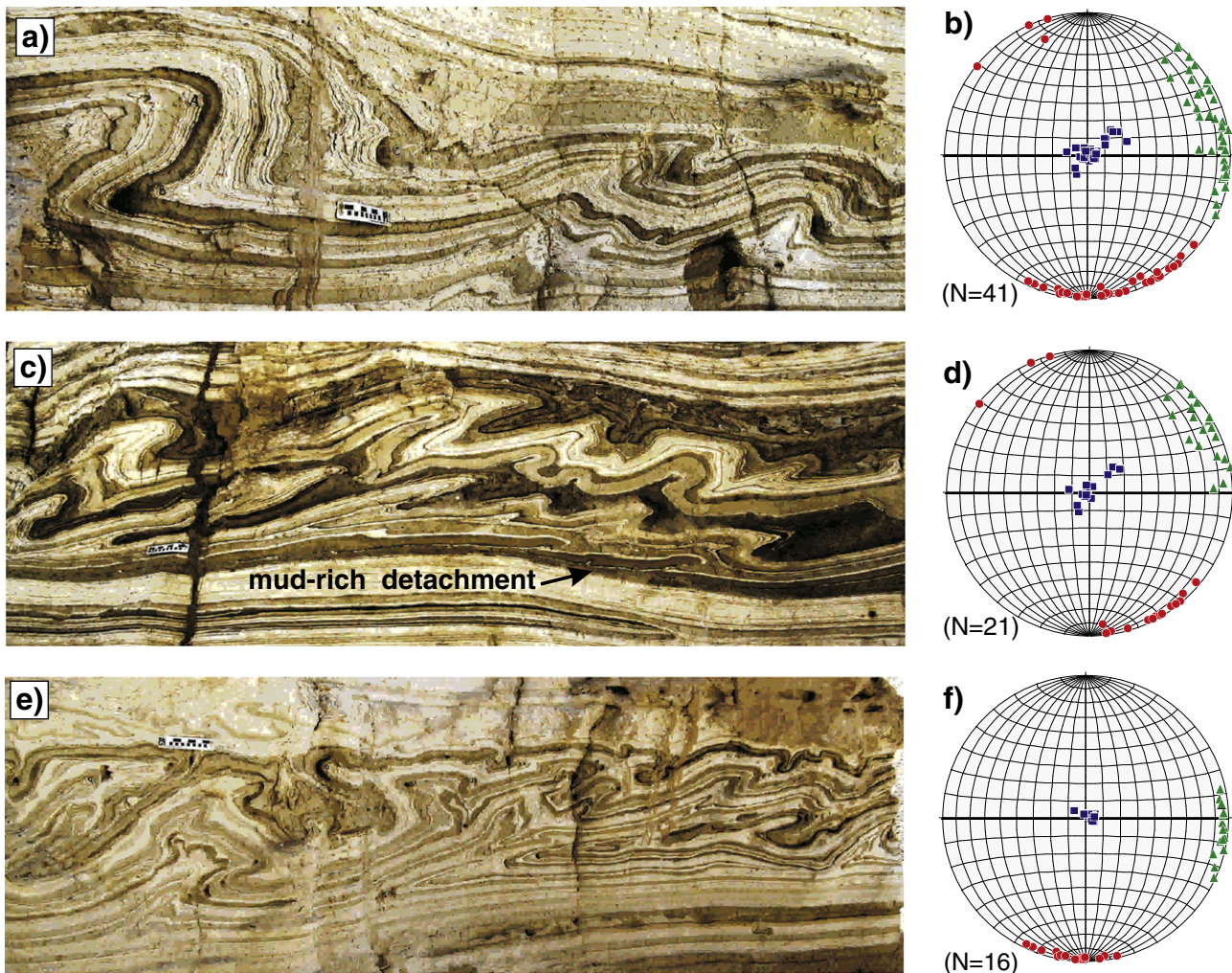


Fig. 8. Sets of representative photographs (a, c, e) and stereonet (b, d, f), from the semi-coherent portions of the case study slump system at Peratzim. Photo (a) and the associated stereonet (b) show overall data from semi-coherent slumps, whilst photos and associated stereonet (c,d) and (e,f) show data from individual structures. Note that in c) the detachment underlying the NE-vergent fold and thrust system locally cuts downward in the downslope direction (below thick light coloured marl). Equal area stereoplots show fold hinges (solid red circles) and poles to the axial surfaces (blue squares). Upward facing directions are projected vertically down (as chordal points) from their upper hemisphere intersection onto the lower hemisphere stereonet (green triangles).

consistently towards the south and southeast (mean $2/165^\circ$) with trends distributed over a 60° arc, although it is notable that semi-coherent slumps display a greater variation *between* adjacent sites (Fig. 8b, d, f). Axial planes typically dip gently to moderately towards the southwest and facing is up towards the ESE (Fig. 8b, d, f). In situations where axial planes are more gently dipping and sub-parallel to the detachment surface, it is apparent that fold hinges are orientated with more NNE–SSW trends (e.g., Fig. 8e, f). This trend is sub-parallel to the inferred downslope direction and indicates that in some cases, there has been a component of fold hinge and axial planar rotations within the more intensely folded parts of semi-coherent slumps. Such rotations are to be expected during intense non-coaxial deformation (see Section 2). We now describe some of the more complex fold geometries that are preserved within semi-coherent portions of slumps.

6.1. Refolded folds

Refolding of cylindrical folds during superposed deformation results in interference patterns that are categorised into 3 main types, depending on the relative orientation of each set of fold hinges and axial planes

(Ramsay, 1967). These patterns assume that both generations of F1 and F2 folds are broadly of the same scale, and that the superposed folds were created by passive shear rather than flexural folding (see Twiss and Moores, 1992, p.255).

6.1.1. Type 1 refold patterns

Type 1 patterns are created where original (F1) and superposed (F2) hinges and axial planes are both normal to one another. The flow direction of the superimposed deformation is close to the axial surface of the original fold, and the section viewed should be normal to this flow direction (Ramsay, 1967 p.520). This arrangement results in classic dome and basin or egg box interference patterns (Fig. 9a). In general the earlier recumbent (F1) folds are tight-isoclinal and are refolded by upright (F2) folds with steep hinges that are open-close in geometry. Although Type 1 patterns are superficially similar to eye-folds generated by sections across the noses of higher strain sheath folds (see Section 7.2 below), we propose that some closed patterns are indeed more akin to Type 1 patterns as they are preserved in relatively low-strain sections of coherent slumps and form a sequence of regular closed patterns (Fig. 9a).

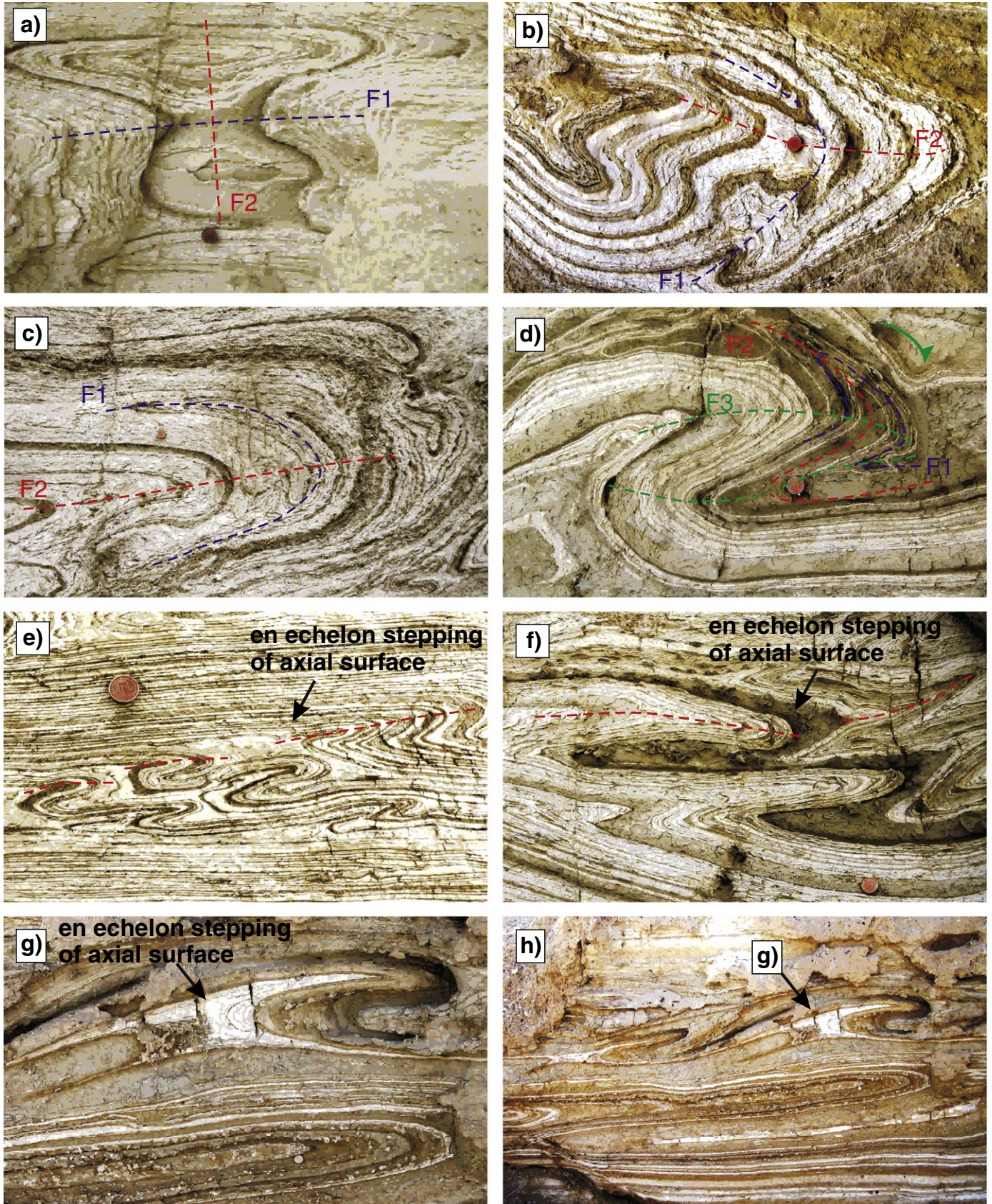


Fig. 9. Photographs (a–d) show Type 1–3 refolds with annotated examples of F1 (blue) and F2 (red) axial planes. a) Type 1 dome and basin fold interference pattern. b) Type 2 mushroom fold interference pattern. c, d) Type 3 hook-shaped fold interference patterns, showing multiple refolded closures (c) and multiple phases of refolding in (d) including F3 axial planes (green). Photographs e–h) show folding with relative attenuation of long limbs and thickening in the hinge and short limb ultimately resulting in X fold geometries (g). In each case, axial planes (highlighted by red dashed lines) display en-echelon stepping across weaker units. Ultimately, X folds form en-echelon fold trains shown in h).

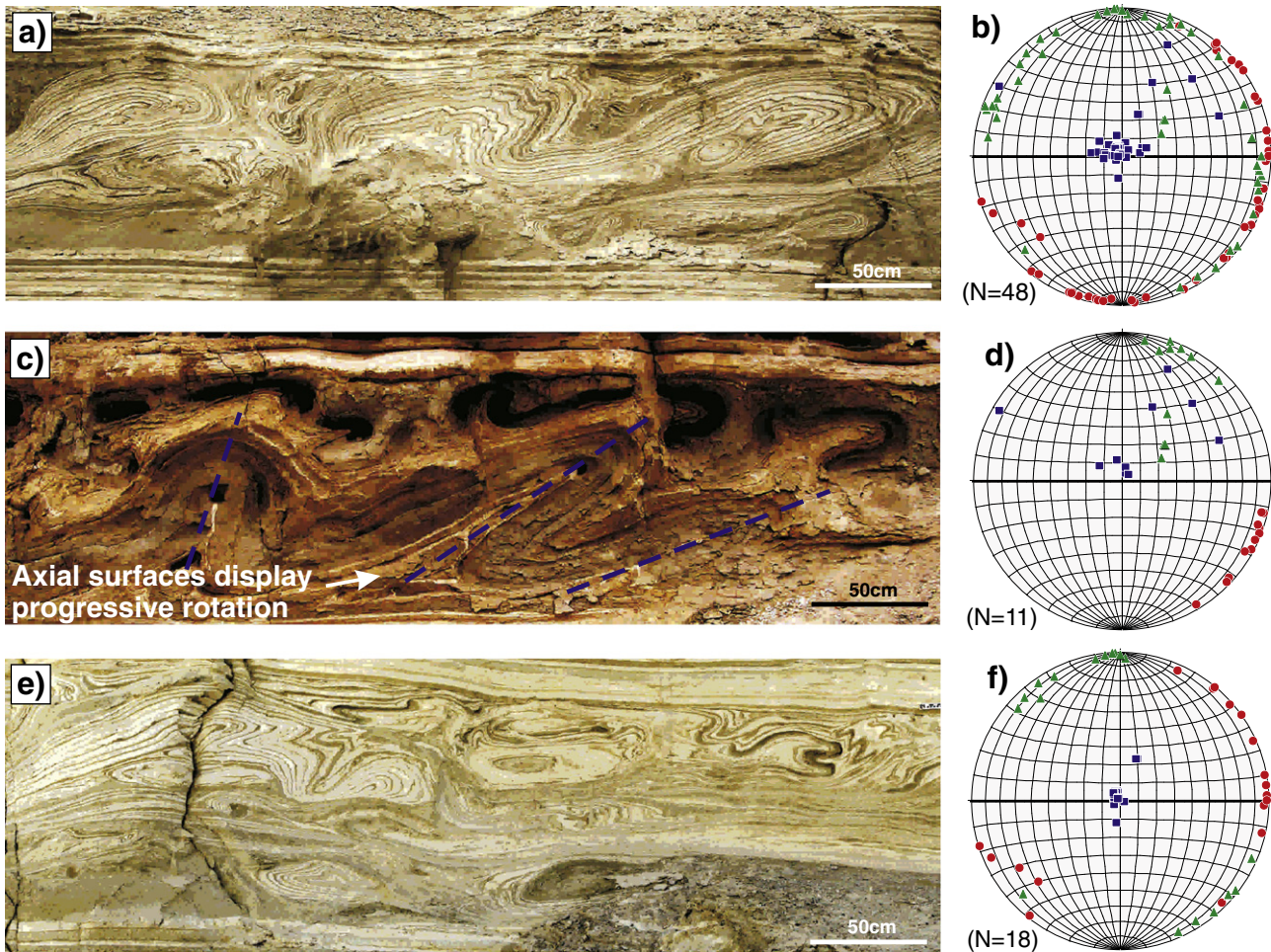


Fig. 10. Sets of representative photographs (a, c, e) and stereonet (b, d, f), from the incoherent portions of the case study slump system at Peratzim. Photo (a) and the associated stereonet (b) show overall data from incoherent slumps, whilst photos and associated stereonets (c,d) and (e,f) show data from individual structures. Equal area stereoplots show fold hinges (solid red circles) and poles to axial surfaces (blue squares). Upward facing directions are projected vertically down (as chordal points) from their upper hemisphere intersection onto the lower hemisphere stereonet (green triangles).

6.1.2. Type 2 refold patterns

Type 2 patterns are created where original and superposed hinges are normal to one another and axial surfaces are also at high angles. The flow direction of the superimposed deformation is at a high angle to the axial surface of the original fold, and the section viewed should be normal to this flow direction (Ramsay, 1967 p.521). These complex patterns are perhaps the most susceptible to slight changes in angles of fold superposition or sectioning resulting in a classic variety of angel wings, mushroom or boomerang interference patterns. Symmetrical forms are created by the 2 sets of folds crossing one another at right angles. Broadly symmetrical forms are locally preserved in the slump with the earlier tight-isoclinal (F1) folds being refolded by more open superposed (F2) folds (Fig. 9b).

6.1.3. Type 3 refold patterns

Type 3 patterns are created where original and superposed hinges are coaxial and axial surfaces are at high angles to one another. The flow direction of the superimposed deformation is at a high angle to the axial surface of the original fold, and the section viewed should be parallel to this flow direction and normal to the axial surface of the superposed

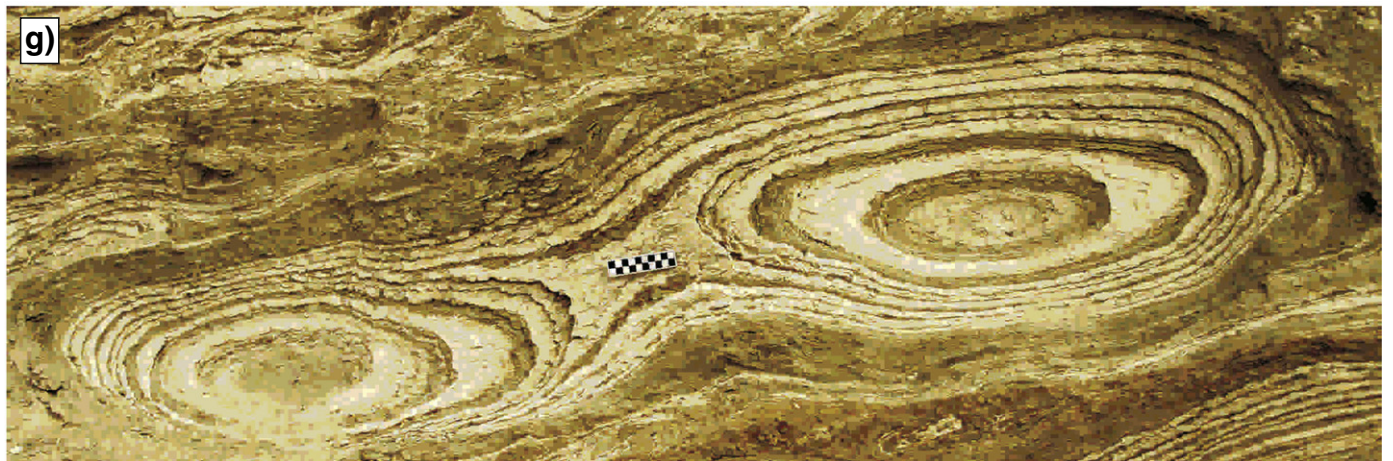
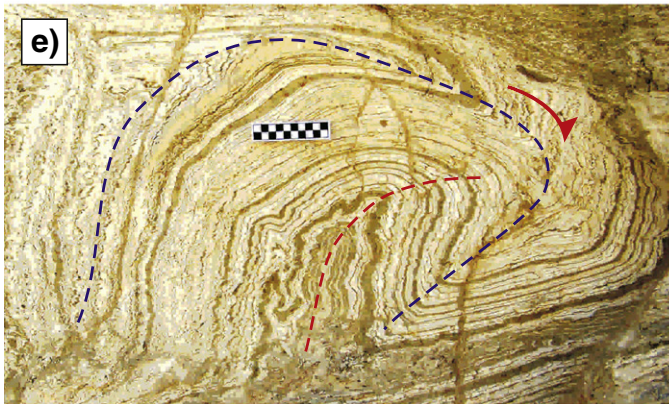
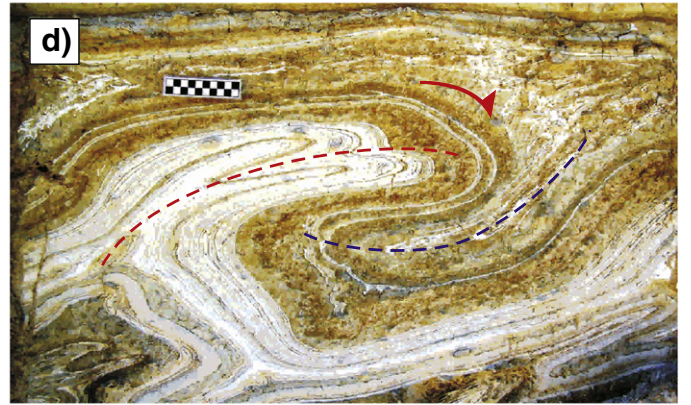
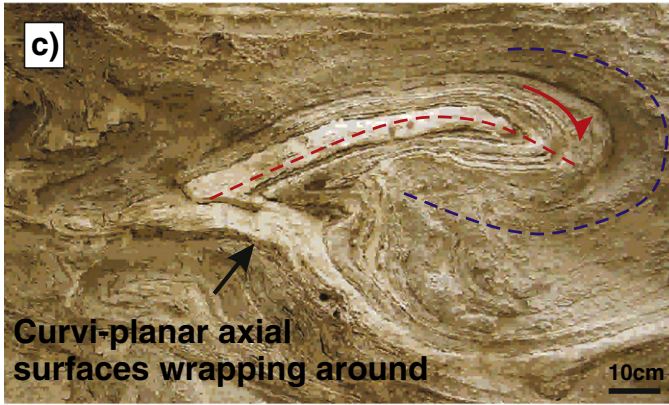
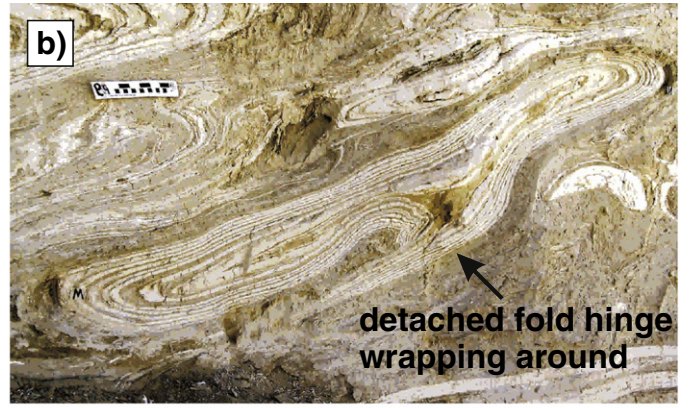
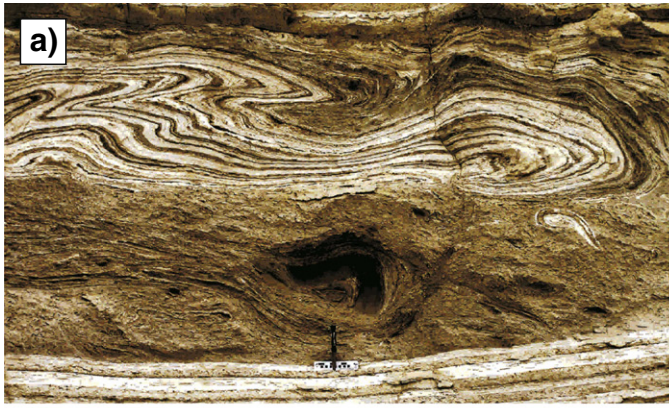
fold (Ramsay, 1967 p.521). This arrangement results in classic hook or fish-hook interference patterns (Fig. 9c, d). Numerous examples of these Type 3 interference patterns are observed on the steep sided walls of wadis where they trend parallel to the NE-directed palaeoslope. In general, these Type 3 refold patterns are only preserved in the hinges of later folds, where the earlier (F1) folds are isoclinal and are refolded by the later close-tight recumbent (F2) folds that verge downslope. In some instances, up to 3 phases of folding are identified, resulting in Type 3 F1–F2 interference patterns that are themselves being refolded by yet later (F3) folds generating complex refolded hook patterns (Fig. 9d).

In summary, these observations of refolded folds collectively indicate that late deformation has to some degree modified the original fold geometry in a two-stage process. In some cases, it is also clear that there had even been multiple phases of refolding (F1–F3) during translation of the slump sheet.

6.2. X folds

When minor folds, that exhibit a buckle fold style in relatively competent layers, are traced along their axial surface they are found

Fig. 11. Representative photographs (a, b) of folds from incoherent portions of slumps. Note that although bedding can be partially traced around folds, the lower fold limbs are frequently attenuated and the folds themselves have become disarticulated and detached. *Spiral folds* (c, d, e) display curved axial surfaces (highlighted by blue and red dashed lines) that are wrapping around one another in sections parallel to transport, whilst *sheath folds* (f) are marked by elliptical eye-fold closures in sections normal to transport. Sheath folds form multiple en-echelon closures that collectively form spectacle shaped eye-fold closures (g).



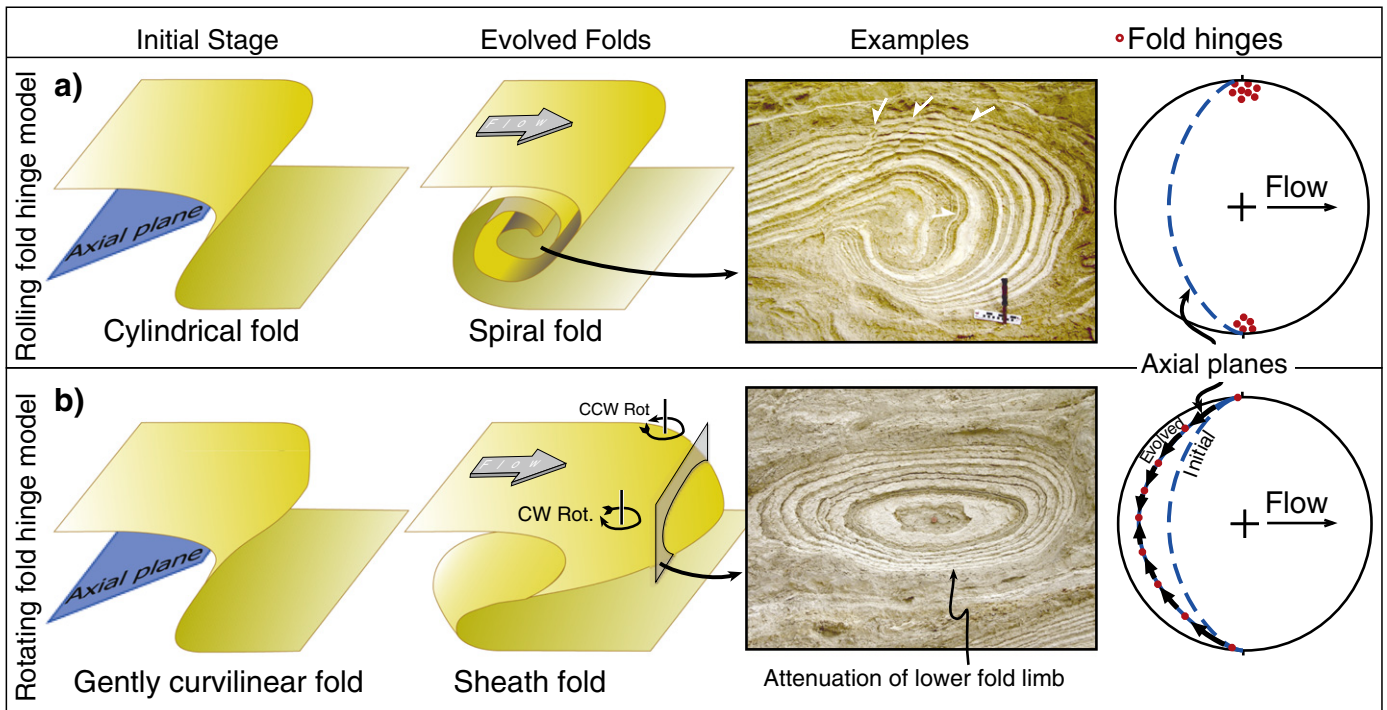


Fig. 12. a) Rolling fold hinge model showing a cylindrical fold in the initial stage evolving into a *spiral fold* whilst maintaining hinges broadly orthogonal to flow/slope direction. The photographic example is from the incoherent portion of the slump system and shows extensional minor faults developing on the upper limb of the spiral which progressively flattens as the fold rolls downslope. A minor thrust is also generated in the hinge of the fold, together with extreme attenuation of the lower fold limb as beds wrap around the spiral hinge. The schematic stereonet shows how fold hinges (red dots) remain normal to the flow/slope direction throughout. b) Rotating fold hinge model showing a gently curvilinear fold in the initial stage evolving into a sheath fold with hinge segments rotating in a clockwise (cw) and counter-clockwise (ccw) sense towards the flow/slope direction. The photographic example from the incoherent portion of the slump system shows a cross section across the nose of a sheath which displays an attenuated lower fold limb. The schematic stereonet shows how fold hinges (red dots) sequentially rotate towards the flow direction as the gently west-dipping axial plane (blue great circle) progressively flattens and rotates toward the sub-horizontal flow/shear plane.

to abruptly migrate laterally or jump when passing through relatively incompetent mud-rich beds (Fig. 9e). This soft-linkage results in axial surfaces twisting, and in some cases competent units on either side of the weaker bed being brought together and grounding on one another (Fig. 9f). Such patterns once again demonstrate the relatively weak nature of the mud-rich units. In extreme cases developed within incoherent slumps, evacuation of weaker material from the long limbs of folds accompanied by a relative thickening in the hinge and short limb may ultimately result in antiformal and synformal closures in more competent material apparently trending directly into one another, whilst closures in the weaker unit form apophyses that eventually pinch out (Fig. 9g). A line joining the tips of each pair of apophyses will provide the relative orientation of the short limb compared to the long limb enabling original fold vergence to still be determined.

Thus, although trains of such structures that we here term *X* folds superficially resemble a form of boudinage, they are considered to be created by folding associated with extreme ductility contrast, with the overall asymmetric pattern still reflecting the original downslope fold vergence (Fig. 9g, h). Heterogeneous layering therefore not only controls local detachments and folding, but will also influence the geometry of individual folds.

7. Observations from intensely deformed incoherent portions of slumps

The intensely deformed portions of slumps are marked by incoherent structures in which bedding has become disarticulated, whilst folds are largely detached and isolated within a fine matrix (Figs. 10a, c, e,

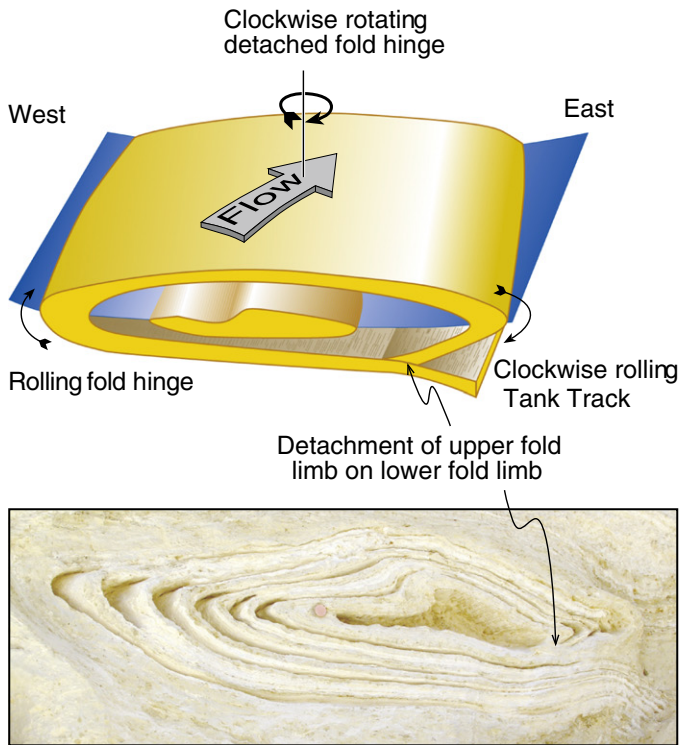
11a, b). Thus, while bedding can be traced around individual folds which in themselves appear relatively coherent, they are completely separated from other structures and the slump therefore lacks overall organisation. Fold hinges are sub-horizontal to gently plunging and collectively form distribution patterns that are widely dispersed over $> 180^\circ$ (Fig. 10b, d, f). It is notable that this pattern does include some hinges that are NNE–SSW trending and parallel to the inferred downslope direction (Fig. 10b). Axial planes are also more variably orientated, although the majority are gentle to sub-horizontal reflecting the recumbent and re-clined nature of folding. Due to the variability of fold hinges and axial planes, calculated facing directions are also distributed around the entire perimeter of the stereonet (Fig. 10b, d, f).

In summary, whilst fold hinges are dispersed around a wide range of orientations when incoherent parts of slumps are viewed as a whole, locally coherent and clustered distribution patterns are preserved around individual hinges (Fig. 10c, d). In some instances, fold hinges are SE-trending at a high angle to the palaeoslope, and display a progressive tightening as axial planes sequentially rotate towards a recumbent attitude sub-parallel to the shear plane (Fig. 10c, d). Some of the complex but still recognisable structures developed locally within incoherent portions of slumps are now described in more detail.

7.1. Spiral folds

Slump folds (as with any fold) are broadly categorised into cylindrical and non-cylindrical depending on the degree of curvilinearity of the fold hinge. However, it is notable that axial surfaces of slump folds can also

a) Rolling cylindrical hinge



b) Rotating curvilinear hinge

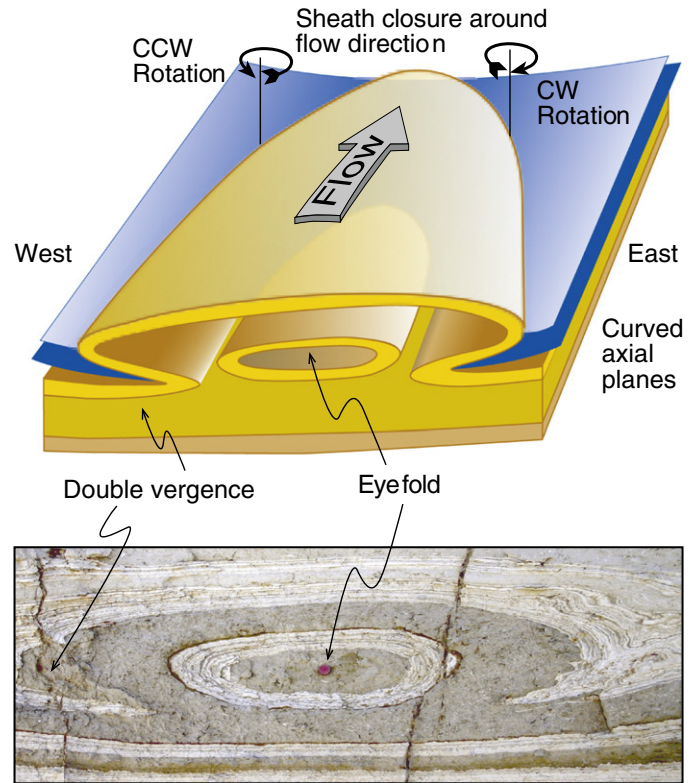


Fig. 13. a) Rolling cylindrical hinge. Photograph and interpretative sketch of a 3-D excavation of a spiral fold from the incoherent portion of the slump system. The spiral fold is completely detached, with the upper fold limb resting directly on the lower fold limb as the fold hinges behave like a clockwise rolling tank track. In addition, both hinges undergo clockwise rotation (in plan view) towards the flow direction. The axial surface of the spiral (shown in blue) is gently curvi-planar. b) Rotating curvilinear hinge. Photograph and interpretative sketch of a cross section across a sheath fold resulting in double vergence and eye-fold sections from the incoherent portion of the slump system. The sheath fold is considered to close around the flow direction, with hinge segments on either side of this direction interpreted to rotate in opposing clockwise and counter-clockwise senses. The axial surface of the sheath (shown in blue) is gently curvi-planar due to non-isoclinal double vergence folds.

become curved, with the axial surfaces of some antiformal and synformal fold pairs apparently wrapping around one another (Fig. 11c, d, e). The sense of wrapping and vorticity is consistent with the top of the fold moving towards the NE and down the palaeoslope (Fig. 11c, d, e). Cylindrical folds within the Lisan Formation are typically asymmetric, with west-dipping axial planes and easterly-directed vergence (Fig. 12a). In a case study example, a NE-verging fold has become disarticulated with extreme attenuation of the lower fold limb (Fig. 12a). Steep extensional faults on the upper fold limb are progressively rotated and flattened around the fold hinge as beds are apparently rolled over the fold hinge in a tank-track fashion (Fig. 12a). Minor thrust faults can also form in the hinge area (see also Farrell and Eaton, 1988). During progressive simple shear associated with downslope directed movement, the initial fold geometry may evolve into this new category of *spiral fold*, which effectively wraps around on itself as it rolls downslope (Figs. 11c, d, e, 12a). The cylindrical fold hinge thus develops a spiral geometry as it rolls downslope, although fold hinges typically maintain high-angles to flow marking the slope direction (Fig. 12a). The original axial plane will thus become highly refolded and coiled on itself, although the general dip of the axial plane will still be towards the original (westerly) direction. In some cases, the rolling fold hinge becomes completely disarticulated such that the cylindrical hinge is interpreted to rotate towards the flow (slope) direction as the tank-track rolls over on itself (Fig. 13a). The upper fold limb is thus detached directly on the lower limb. Whilst these newly recognised *spiral folds* can superficially resemble sheath folds described below (Section 7.2), the detachment of one limb from the other demonstrates that they do not form complete elliptical closures characteristic of classic eye-fold sections across sheath folds.

7.2. Sheath folds

Within the Lisan Formation, cross sections through curvilinear sheath folds are marked by characteristic eye-fold patterns (e.g., Fig. 11f, g). Gently curvilinear non-cylindrical folds are generally asymmetric and verge towards the east with west-dipping axial planes (Fig. 12b). Gently curvilinear folds are considered to evolve into highly curvilinear sheath folds via a hinge rotation towards the flow (slope) direction during progressive simple shear (Figs. 11f, g, 12b) (Alsop and Carreras, 2007; Alsop and Marco, 2011; Pisarska-Jamrozý and Weckwerth, 2012). Due to the initial gentle curvilinearity of the fold, either end of the hinge will rotate in opposing senses (clockwise and counter/anti clockwise) towards the flow direction (Fig. 12b). Evolved sheath folds will thus display hinges that are distributed along a stereographic great circle marking the axial plane (Fig. 12b). The axial plane itself rotates and flattens towards the sub-horizontal shear plane during progressive simple shear deformation. In detail, the axial planes of evolved sheath folds are gently curvi-planar, and this reflects a geometric necessity of non-isoclinal double vergence folds around sheath folds (Alsop and Holdsworth, 2007) (Fig. 13b). Cross sections normal to the flow direction display such double-vergence geometries and also cut through the nose of the sheath to reveal concentric elliptical eye-fold patterns. Such eye-folds frequently display attenuation of the lower fold limb (Fossen and Rykkeldid, 1990), although sheaths that originate as upright buckles may actually retain a thicker lower limb (see Section 5.2.) (Fig. 7a,b). Multiple sheath folds can define en-echelon patterns that collectively form spectacle eye-folds (Fig. 11g). The elliptical ratios of the closed rings have been used to determine the bulk strain regime (Fig. 13b). Comparing the

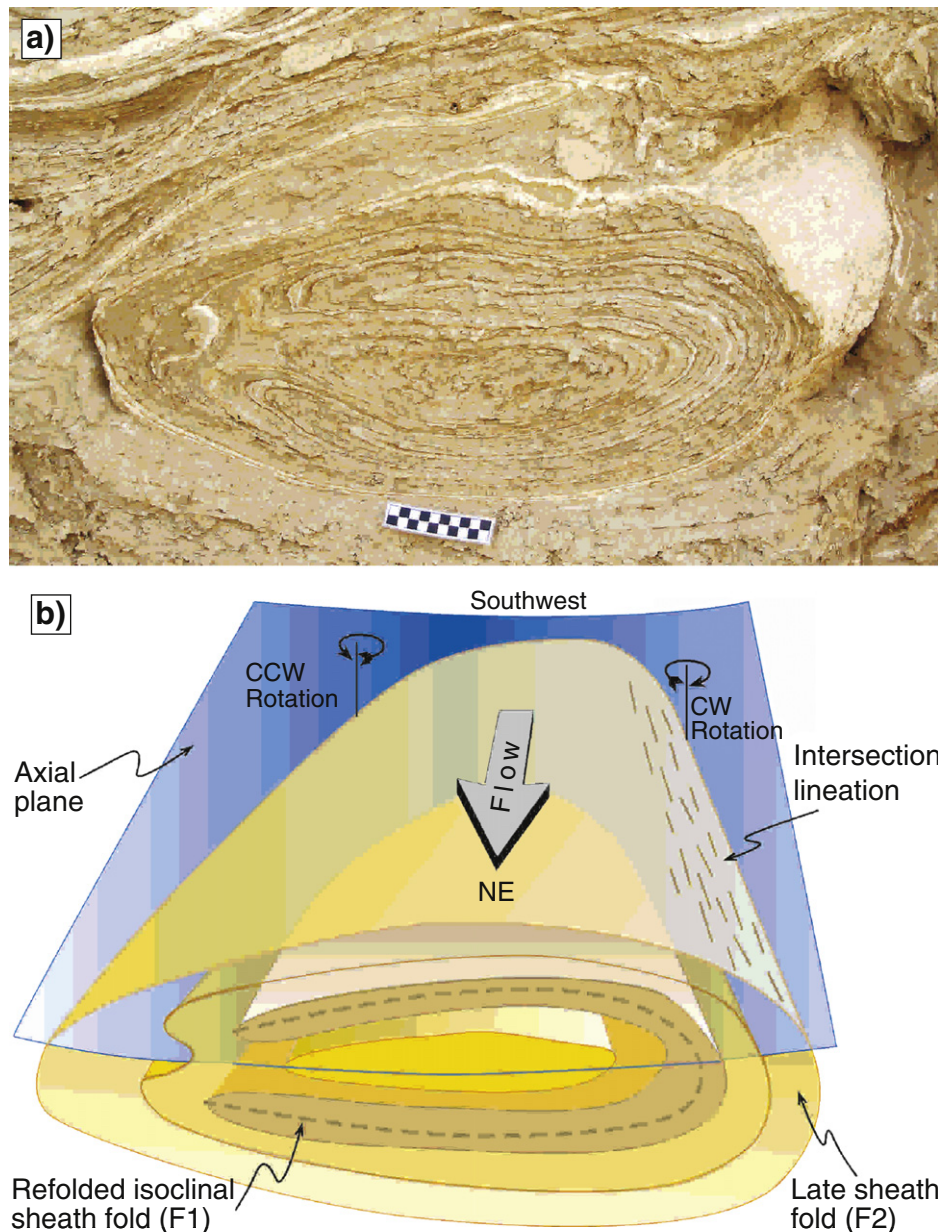


Fig. 14. Photograph (a) and interpretative 3-D sketch (b) of a refolded sheath fold from within the incoherent portion of the slump system at Peratzim. The early (F1) sheath fold has been refolded around the later (F2) sheath axial plane to define a completely enclosed refold pattern.

elliptical ratios of the outermost and innermost eyes (see [Alsop and Holdsworth, 2007, 2012](#); [Alsop et al., 2007](#) for details of the technique) produces elliptical ratios of $R' = 0.93$ and $R' = 0.85$ in [Figs. 12b](#) and [13b](#) respectively. These values are consistent with eye folds associated with general shear, where simple shear is combined with a flattening component (possibly associated with a subsequent slight compaction). Such patterns are widely developed in sheath folds formed during gravity-driven soft sediment deformation associated with slumping (see [Alsop et al., 2007](#)).

7.3. Refolded sheath folds

Highly curvilinear sheath folds forming eye-folds in y - z cross section may themselves be refolded by subsequent sheaths (e.g., [Fig. 14a](#)). Refolded sheath folds are marked by early eye-folds (F1) that are

isoclinally refolded and entirely enclosed within the later (F2) sheath eye-fold. This relationship results in coaxial F1 and F2 fold hinges that are sub-parallel to intersection lineations formed around exposed bedding planes ([Fig. 14b](#)). Excavated fold hinges are NE trending and sub-parallel to the inferred flow (downslope) direction. This geometric relationship is consistent with progressive deformation associated with the same NE-directed slope direction. The fact that the early (F1) sheaths have been refolded indicates that the flow became unsteady and deviated, or that the development of the sheath itself caused a local perturbation in the orientation of layering relative to flow leading to refolding. Similar refolded sheath folds have also been observed on a large-scale in mid-crustal metamorphic terranes (e.g., [Alsop, 1994](#)). It is notable that some of the best-preserved examples of sheath folds are synformal closures representing the return hinges of fold pairs. This is interpreted to reflect the role of active folding, where the mechanically

stronger layers forming the preserved fold are more easily dragged into sheath geometries as surrounding weaker units are translated in the flow direction (see Alsop and Holdsworth, 2012).

Thus, although incoherent slumps have in the past been described as “chaotic” which is defined as “complete disorder and utter confusion” (Collins English Dictionary & Thesaurus, 2000) it is apparent to us that a degree of order can still be deciphered from within the majority of the system. Clearly, as with interpretation of most natural systems, the degree of incoherence identified in a system is partially influenced by the scale at which observations are integrated. However, breccia layers that display more chaotic fabrics are developed locally at the top of some slump sheets, and are previously interpreted as recording earthquakes and associated seiche events (e.g., Agnon et al., 2006; Alsop and Marco, 2012b; Marco and Agnon, 1995). Such breccia layers may represent the most extreme form of deformation, where simple folds have evolved through coherent vortices into turbulent and chaotic structures such as breccia (e.g., Heifetz et al., 2005; Wetzler et al., 2009).

8. Discussion

The intensity of deformation observed at Peratzim is considered to broadly increase from coherent through to incoherent portions of slumps. Structures formed when a slump was acting as a mechanically coherent or semi-coherent mass can still be preserved within isolated rafts when it is behaving as a largely incoherent body, indicating that the coherent portions of slumps may ultimately evolve into incoherent. The exact style of deformation in any portion of the slump will clearly

depend on the nature of material being deformed, reflecting variables such as lithology, cohesiveness, mechanical heterogeneity, multilayering and fluid pressures, etc. (see reviews in Maltman, 1994a,b,c). We now discuss in more detail some of the major issues and questions that have been raised during this study.

8.1. How can gravity-driven slumping occur down exceptionally gentle (<1°) slopes?

The Lisan Formation exposed along the western shore of the Dead Sea and in the case study area of Peratzim displays extremely low dips of <1° (Alsop and Marco, 2011). Despite, the sub-horizontal attitude of the beds, associated slumps display consistent (>90%) vergence and overturning towards the Dead Sea Basin, implying that even a minimal slope is capable of controlling slumping (Alsop and Marco, 2011, 2012a,b). Some of the significant factors influencing slope failure and slump development on very gentle slopes are outlined below.

8.1.1. Angle of the slope

Gravity-driven shearing is typically considered to be the primary mechanism of slump sheet movement, with the maximum principal shear stress interpreted to be parallel to the slope (e.g., Strachan, 2002 and references therein). Although, extremely gentle slopes of <1° will only generate very low shear stresses, slumping is still recorded in subaqueous environments at these angles (e.g., Field et al., 1982; Garcia-Tortosa et al., 2011). This indicates that the angle of slope is

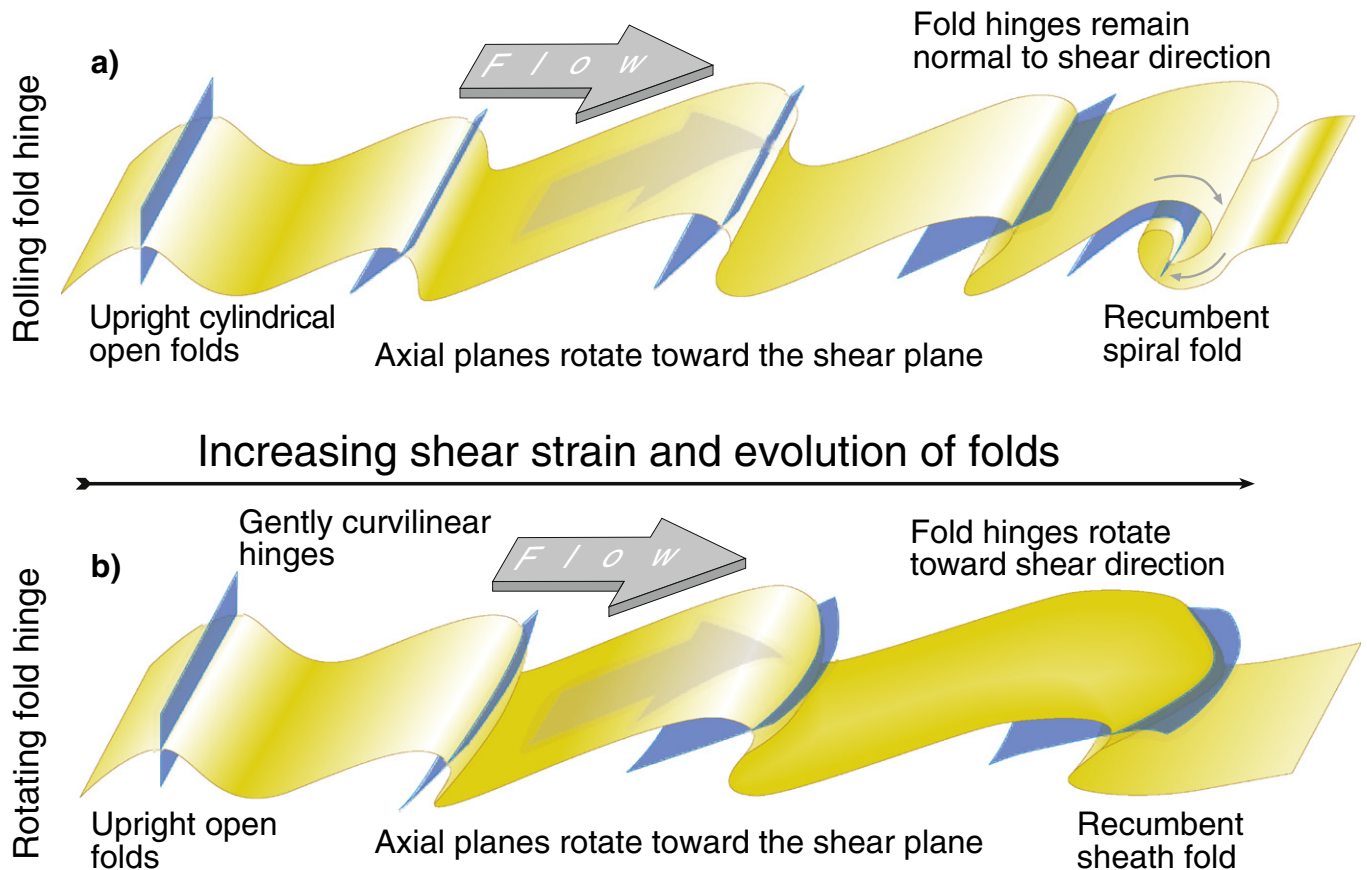


Fig. 15. a) Rolling fold hinge model showing open, upright cylindrical folds developed normal to flow. With increasing shear strain (towards the right of the figure), the folds progressively evolve with axial planes (shown in blue) sequentially rotating and flattening towards the flow plane to generate recumbent spiral folds. These folds are associated with clockwise (as viewed) spinning hinges maintaining high angles to flow. b) Rotating fold hinge model showing open, upright gently curvilinear folds developed broadly normal to flow. With increasing shear strain, the folds progressively evolve with axial planes sequentially rotating and flattening towards the flow plane to generate recumbent sheath folds. These folds are associated with fold hinge segments rotating towards the shear/flow direction.

not the only control on slumping, and that other factors must influence the process.

8.1.2. Pore fluid pressures

It has long been realised that one of the most effective mechanisms to reduce the shear strength of sediments, and thereby encourage and facilitate their failure, is to increase pore fluid pressure (e.g., Maltman, 1994a,b,c and references therein). Pore fluid pressures within sediments will be increased by seismic waves generated during earthquakes, thereby resulting in the initial slope failure. However, as the resulting slump sheet translates downslope, it will locally increase the loading on underlying sediments thereby also increasing pore fluid pressure and encouraging further movement and further deformation (e.g., Strachan, 2002).

8.1.3. Layer-cake stratigraphy

Failure associated with slumping down extremely low angle slopes ($<1^\circ$) has been recorded from a number of Pleistocene lacustrine environments (e.g., Garcia-Tortosa et al., 2011; Gilbert et al., 2005). We propose that varve-like layering within lacustrine settings will facilitate slumping as: a) alternating layers of different compositions may naturally act as seals and trap pore fluids; and b) sub-horizontal layers potentially provide numerous sub-parallel slip surfaces that are unhindered by depositional irregularities associated with sediment thickness changes.

Within the Lisan Formation of the case study area, the recognition that many slumps detach in, or just above, clastic and mud-rich horizons implies that fluids trapped within these units play a significant role in the slumping process. The possibility that mud and clastic rich horizons were saturated with water is consistent with the view that they were rapidly deposited, and hence trapped interstitial water, during winter storm events (Alsop and Marco, 2011; Begin et al., 1974). The potential presence and role of fluids within clastic-rich horizons is supported by: a) upright billow folds are observed within thicker mud-rich units, and these have been interpreted as being created via density-driven perturbations associated with Rayleigh–Taylor instabilities during the initial seismic event (Alsop and Marco, 2011); b) upright folds overturning in opposing directions have been interpreted as reflecting dewatering during seismicity (e.g., Fig 7f, Alsop and Marco, 2012b); and c) slump sheets are cut by numerous sedimentary dykes containing sediment infill interpreted to have been transported and deposited when underlying mud-rich units became fluidised (Levi et al., 2006). In summary, increases in pore fluid pressure triggered by seismicity and translation of slump sheets, coupled with the exceptional layer cake stratigraphy deposited in the lacustrine environment, are considered to be the major factors facilitating failure and slumping on very gentle slopes such as preserved around the Dead Sea Basin.

8.2. How do classical re-fold patterns form almost instantaneously within slumps?

The fact that different re-fold types (e.g., Ramsay, 1967) are observed within an individual slump sheet implies that they were created during a single progressive deformation, rather than multiple phases of punctuated deformation (Fig. 9a–d). Different re-fold patterns indicate that fold hinges and axial planes sequentially form at different angles to one another thereby creating Types 1–3 interference patterns. Folds can form at different angles to one another within a single deformation associated with a uniform slope direction due to a) folds initiating at different angles, and b) earlier folds rotating into new orientations prior to initiation of later folds (e.g., Ortner, 2007). Within metamorphic terranes such archetypal refolding has been traditionally interpreted as being created by multiple phases of punctuated deformation (see Ramsay, 1967). The fact that the full range of classical re-fold scenarios are observed entirely within a single slump horizon indicates that such geometries can indeed be potentially generated during a single progressive deformation.

8.3. Why do some fold hinges rotate and others roll during slumping?

Fold hinges within slump systems, and other high strain settings, frequently rotate towards the transport direction resulting in hinges which are variably orientated along the axial plane ultimately resulting in sheath fold geometries (Fig. 15a, b) (Alsop and Carreras, 2007). However, in the Dead Sea case study, the stereoplots of fold hinges from coherent and semi-coherent portions of slumps show clustered patterns, with only very limited evidence of systematic hinge dispersal along the axial surface reflecting fold rotation. Fold hinges can even remain at high angles to the inferred palaeoslope direction within the incoherent parts of the slumps. In summary, many folds fail to evolve into fully developed sheath folds as observed in other slumps, but display *spiral fold* geometries (Fig. 15a, b) (e.g., Strachan and Alsop, 2006). This may reflect a variety of factors including those detailed below.

8.3.1. Limited deformation and translation of the slump sheet

Sheath folds are typically considered to require high shear strains ($\gamma > 10$) to encourage fold hinges to rotate into the flow direction (see Alsop and Holdsworth, 2007, 2012). Limited shear strain will therefore be insufficient to generate hinge rotation and hence sheath formation. However, within the case study, folds are well developed and isoclinal in places suggesting that shear strain would indeed be sufficient to generate sheath folds. In addition McClelland et al. (2011) recently report that more limited shear strains ($\gamma > 1$) could even be sufficient to create sheath fold structures within sediments if the precursor feature is itself originally gently curvilinear.

8.3.2. Unsuitable deformation dominated by flattening strains

It has been shown that deformation dominated by flattening strains is less likely to encourage fold hinge rotation and can therefore be considered unsuitable for sheath fold development (e.g., see Alsop et al., 2007; Jiang and Williams, 1999 and references therein). However, downslope translations are typically regarded as being dominated by non-coaxial deformation (e.g., Dasgupta, 2008; Woodcock, 1979) which should therefore facilitate sheath formation. It is also noteworthy that within the case study area, the presence of syn-slumping conjugate fault systems striking sub-parallel to flow indicates that a component of non-plane strain deformation has occurred (e.g., Alsop and Marco, 2011).

8.3.3. Variable lithologies encouraging high strain rates

Variable lithologies encourage mechanical heterogeneity within the deforming system that will encourage rolling rather than rotation of fold hinges. Fold hinges within heterogeneous layers may disarticulate from their limbs and become rootless cylindrical folds. These folds typically maintain their high angles to the slope and simply roll as detached cylindrical hinges, resulting in coaxial fish-hook re-fold patterns. In some instances, the detached rolling hinges are interpreted to then rotate as an entity towards the slump direction (Fig. 13a).

8.3.4. Fold hinges contained within the shear plane

Theoretical studies have demonstrated that if a fold hinge, which is interpreted as a line, is contained within the shear plane during simple shear deformation, it will not rotate towards the shear direction no matter how great the deformation (e.g., see Passchier and Trouw, 2005). Within the study area, extremely gentle slopes and sub-horizontal layering in the Lisan Formation ($<1^\circ$) will combine to encourage fold hinges to effectively lie in the sub-horizontal shear plane. Such fold hinges will therefore not rotate towards the shear direction to create sheath folds as deformation intensifies, but rather roll downslope to create spiral folds.

8.3.5. Fold hinges are constrained by layer orientation

Cylindrical fold hinges can display uniform orientations because folds form perpendicular to the direction of shortening *within* a given layer (see Flinn, 1962; Treagus and Treagus, 1981). Bedding which is

oblique to the axes of the bulk strain ellipsoid will generate fold hinges that initiate perpendicular to the direction of shortening *within* that layer (see Flinn, 1962; Treagus and Treagus, 1981). The orientation and geometry of such fold hinges are therefore controlled by relative obliquity between bedding and the strain ellipse. As the strike of sub-horizontal bedding and the trend/strike of the gentle palaeoslope, which controls the finite strain ellipse, are equivalent to one another, then folding more typically initiates parallel to the Y axis within the shear plane. In such cases, it will therefore not rotate towards the X direction during continuing simple-shear dominated deformation (Fig. 15a).

In summary, the strike and dip of the layering are controlled by the same palaeoslope that governs slumping and movement direction (i.e., $X > Y > Z$ of the strain ellipsoid). X lies down the dip of the palaeoslope and Y forms parallel to palaeostrike. This means that folds which form parallel to the palaeoslope (Y) will not rotate. We therefore propose that the pronounced layer-cake stratigraphy, which mirrors the uniform downslope shear direction, constrains folding orientations and style over considerable areas.

8.4. Why do fold hinges define scattered patterns with increasing deformation?

Structural analysis within metamorphic terranes demonstrates that fold hinges can progressively rotate towards the transport or flow direction as deformation intensifies over the scale of kms (e.g., Alsop, 1992; Alsop et al., 2010; Escher and Watterson, 1974). Such distributions have been theoretically modelled and described in terms of fabric attractors (Passchier and Trouw, 2005). However, in this example, the distribution of fabric elements such as fold hinges and axial planes actually becomes more scattered as deformation increases from coherent to incoherent settings. This may reflect the interplay of a number of variables listed below.

8.4.1. Folds initiate on variable slopes

Folds can be expected to have variable orientations if the slope upon which they formed was also variable. In a recent study, sub-lacustrine landslides from within volcanic crater lakes are marked by slope failures that converge towards the centre of the basin (Moernaut and De Batist, 2011). Slumped units extend for up to 500 m and develop on palaeoslopes with dips of $\sim 2^\circ$ to form a coherent radial system. On a regional scale within the Lisan Formation, the slopes around the Dead Sea Basin are variably orientated, and result in a radial convergent pattern of slumps directed towards the deepest part of the Dead Sea (that also coincides with the depocentre of Lake Lisan) (Alsop and Marco, 2012b). Within the case study example at Peratzim however, there is no evidence of variable slopes as folds generated in the coherent portions of slumps display uniform and consistent orientations (see Section 5). In addition the collection of data from a relatively small area comprising just ~ 250 m across the strike of the slumped unit would tend to preclude significant variation.

8.4.2. Folds initiate at different times

As noted above, fold hinges will typically rotate towards the slope/flow direction whilst axial planes rotate towards the shear plane during intense non coaxial deformation. Folds that initiate earlier in the history of progressive deformation will therefore be expected to have undergone greater amounts of rotation compared to those folds that form late in the sequence. Whilst this could influence some fold patterns, it should be noted that in this case study all folds are created within a single progressive slump event. As this slump event may last just a matter of minutes (e.g., Alsop and Marco, 2012b) there is only a limited time for a systematic series of new structures to develop.

8.4.3. Folds initiate in different orientations

Slump folds will theoretically initiate in a whole range of orientations depending on if velocity gradients across the failure surface are

greatest in the downslope direction, or alternatively along strike towards the margins of the slump (see Alsop and Marco, 2011). Folds will initiate at high angles to flow when layer-parallel shear dominates and velocity gradients are greatest down the slope, whilst layer-normal shearing associated with along strike differential shear will generate folds that initiate oblique of even sub-parallel to the downslope direction. Within this case study, folds measured in coherent portions of slumps are uniformly SE-trending and are therefore consistently at high-angles to the NE-directed palaeoslope (Alsop and Marco, 2012a). If we assume that coherent portions of slumps may ultimately evolve into the incoherent, then it is clear that folds did not initiate at variable angles to flow but rather formed consistent orientations at high angles to the downslope direction.

8.4.4. Folds are refolded into different orientations

Distinct patterns of refolding are recognised in many metamorphic terranes and shear zones. Within this case study Type 1 dome and basin, Type 2 angel wings and Type 3 hooked interference patterns have all been recognised from within the slumped horizon. Such refolding associated with Types 1 and 2 will locally reorientate the earlier fold hinges, although the more common Type 3 is associated with coaxial hinges and therefore will not markedly influence the trends of pre-existing hinges. Within the slumped unit, there is no evidence of overprinting by deformation associated with adjacent slumps (see Alsop and Marco, 2011). In addition, although refolding is clearly observed it is not ubiquitous and we therefore suggest that refolding does not play a major role in scattering fold orientations within incoherent slumps.

8.4.5. Folds rotate at different rates

Theoretical work on non-coaxial flow has demonstrated that folds forming greater angles to shear will rotate more rapidly than those which are sub-parallel to flow (see Passchier and Trouw, 2005). Variable rates of rotation will lead to scatter of fold hinges if they formed at slightly different times and/or orientations. In addition, hinge rotations may be facilitated within incoherent slumps, where folds have become detached and disarticulated from adjacent structures. This allows folds to rotate as individual entities that can behave differently to adjacent (but now unrelated) structures. Such disarticulation resulting in well-formed folds floating in the surrounding fine grained matrix permits spiral folds to fully develop, and may have a significant role to play in generating folds at a variety of orientations within incoherent slumps.

In summary, the orientation of the final fold population within incoherent slumps is probably a composite distribution influenced by a range of these variables. All of these are affected by the exact nature of deforming material in terms of thickness of multilayers, and the effect of these on the mechanics of deformation. The overall breaking-down of aragonite-mud laminae from coherent to incoherent slumps will obviously weaken the slumped mass, as well as release pore fluids within the slump. These temporary increases in pore fluid pressure can significantly affect the behaviour of the slump, although they could leave little tangible evidence of their role in this process. An understanding of the development of folds from coherent to incoherent slumps is important when using associated folds to determine the orientation of palaeoslopes (see Alsop and Marco, 2012a; Debacker et al., 2001, 2009; Strachan and Alsop, 2006 for reviews). The present study demonstrates that folds from coherent slumps are most reliable for palaeoslope analysis, whilst those from more incoherent slumps are problematic due to disarticulation resulting in a rotation of large, but apparently still intact, hinges.

8.5. Why do axial surfaces in some slump folds define en-echelon patterns as they step across weaker units?

Buckle folds formed within relatively competent beds are observed to migrate laterally across weaker units in multilayer sequences, due to thinning of long limbs and thickening of hinges and short limbs

(Fig. 9e–h). The net effect of this is for associated axial planes to be marked by relative jumps across the incompetent unit typically defined by muds (Fig. 9f). In extreme cases, fold trains are modified into a series of newly classified en-echelon X folds that still broadly verge in the direction of shear. The geometry of the X folds is considered to be controlled by a number of variables listed below.

8.5.1. Orientation of initial folds

Within zones of intense non-coaxial shear developed in gravity-driven slump sheets, thickening or thinning of fold limbs reflects the orientation of the initial fold relative to the shear plane (Fig. 7a–d). Relative thinning of long limbs and thickening of the hinge and short limbs indicates that X folds initiate as upright folds rather than monoforms (see Section 5.2).

8.5.2. Geometry of initial folds

X folds can only develop where the vergence of the initial fold is in the same sense as the intense shear that subsequently effects the fold. An application of intense non-coaxial shear to inclined or overturned folds with an opposite sense of vergence may simply lead to an unfolding or opening of the fold pair (e.g., see Sengupta et al., 2005) and the characteristic apophyses of X folds will fail to develop. X folds are therefore most likely to develop where the initial folds form in the early stages of progressive deformation, and are sequentially sheared out during continued slumping.

8.5.3. Extreme ductility of layers

The degree of attenuation required to create X fold geometries, where even the outer-arcs of hinges in competent layers are reduced to apophyses, indicates that layering must be extremely ductile (Fig. 9g, h). Whilst this can be achieved within water-rich unlithified sediments by dramatic increases in pore fluid pressure, we believe that equivalent structures have not been identified and described in detail from metamorphic rocks, suggesting that the requisite conditions are not so readily attained.

8.6. Why do parasitic folds rarely develop around slump folds?

Folds in many metamorphic rocks are associated with smaller (2nd order) folds that are considered broadly coeval with the larger fold, and whose asymmetry switches as they pass around the hinge of the larger fold (e.g., Fossen, 2010). The vergence of such parasitic folds is frequently used to determine the position and geometry of the larger folds, and has proved to be a useful tool when working in metamorphic terranes. However, despite the plethora of well-exposed slump folds within the Lisan Formation, parasitic folds so characteristic of folds in metamorphic rocks are typically lacking and this issue is discussed below.

The theory behind controls on folding has been discussed at length and includes factors such as viscosity ratio between layers, anisotropy, together with thickness and spacing of layers of different competences (see a recent review by Hudleston and Treagus, 2010). Whether layers in a system are folding independently, or behaving as a multilayer package is determined by the layer spacing in relation to the dominant fold wavelength (Hudleston and Treagus, 2010). When the layer spacing is greater than the single layer dominant wavelength then individual layers behave independently, whereas closer spacing results in all layers forming a multilayer package. Different models exist to explain the development of small parasitic folds around larger folds. Frehner and Schmalholtz (2006) propose that minor (parasitic) folds that are developed in thin layers grow more quickly than larger folds (in thicker layers) as initial layer irregularities are more important in initiating and growing folds in the thinner layers. Alternatively, Treagus and Fletcher (2009) suggest that parasitic folds are more likely to develop if the thin layer is the most competent of all layers, or if the whole multilayer is narrowly confined above and below by stiffer more competent units.

The general lack of parasitic folds in the slump setting therefore reflects the fact that: a) slump folds form many orders of magnitude more rapidly than equivalent metamorphic folds, perhaps in a matter of just a few minutes in the case of the Lisan Formation. There is therefore a very limited opportunity for folds to initiate and grow at different times/rates. b) Although differences in competence clearly exist within slump folds (creating the characteristic buckle fold patterns in some units), the competency contrast between the thinner layers (typically aragonite-rich) and surrounding mud-rich layers may not be great enough to create parasitic folds. This is also demonstrated within slumps by the limited occurrence of boudinage that requires marked viscosity contrasts. Perhaps most importantly, many slumps form part of a surficial or opencast process meaning that they are not significantly confined by more competent overlying beds. In summary, the typical lack of parasitic folds around the studied slump folds may simply reflect the rapid rates of deformation, more limited competency contrasts and lack of a confining overburden compared to many metamorphic rocks.

8.7. How representative and useful are structures formed in recent low angle slumps when interpreting those preserved in the geological record?

It is an intriguing puzzle as to why the preservation of structures associated with very low angle (<1°) slope failures appears to be limited in the geological record. Most authors who have worked on older systems suggest that more significant slopes are required to generate slumps (e.g., Allen, 1982; Lewis, 1971) although van Loon et al. (2012) have recently suggested that such low angle systems resulting in the sliding of brecciated blocks may indeed have operated in the Cambrian. Clearly, very low angle subaqueous failures do occur in more recent and modern settings (e.g., Field et al., 1982; Wells et al., 1980), and experiments have also demonstrated that movement can occur down very low angle slopes (e.g., Owen, 1996). The relative lack of low angle slope failures and slumps in the geological record may therefore reflect not only the increased likelihood of subsequent tectonics, tilting, and variable compaction rendering accurate measurement of subtle (<1°) slopes very difficult in ancient settings, but also the inherent preservation potential of such structures.

The chances of preserving low angle slumps will depend on a variety of factors including the gross sedimentary environment in which the slump occurs. Very low angle slope failures have been recorded in a number of lacustrine settings where seismicity triggers the slope failure (e.g., Alsop and Marco, 2011, 2012b; Garcia-Tortosa et al., 2011; Gilbert et al., 2005). The tectonically active nature of these settings may however ultimately limit their preservation potential. Other exceptionally gentle slope failures of just 0.25° occur within tidal flats (Wells et al., 1980) that also have a limited preservation potential as shorelines are relatively transient and occupy a very small percentage of global surface area. Therefore although low angle slope failures clearly operate today and pose a viable risk to hydrocarbon infrastructure, their potential for preservation is perhaps limited unless we can recognise any deeper water effects of such failures and thereby fingerprint them in the geological record.

Despite the potentially limited opportunity for the preservation of low angle recent slumps noted above, the observation and analysis of such systems is still extremely useful when attempting to interpret those older structures now preserved in lithified rocks. The advantages of working in relatively recent (unlithified) slumps such as those formed in the Lisan Formation exposed around the Dead Sea Basin are that a) potential ambiguities relating to 3-D geometries can be largely removed via careful excavation, b) exposures are typically continuous thereby permitting adjacent structures to be more easily and fully integrated across a range of scales, c) gross controls on kinematics such as slope angles and orientations are clearly visible, thereby reducing potential inaccuracies in older settings where original slope attitudes can only be inferred. The potential uncertainties noted above typically multiply when dealing with

older rocks that have themselves been subsequently tectonised and tilted (e.g., Ortner, 2007; Waldron and Gagnon, 2011). Thus, an analysis of structures in recent settings allows concepts and models of slumping and slope failure to be more rigorously tested, as fewer variables and unknowns exist.

9. Conclusions

In summary, frameworks established for the geometric analysis of folds and fabrics in metamorphic rocks can be successfully applied to structures generated during gravity-driven soft-sediment deformation on very gentle ($<1^\circ$) slopes. The general classification of portions of a slump into coherent, semi-coherent and incoherent is based purely on the preserved geometries and is thought to reflect the finite state of deformation within the slump. This classification does not refer to the temporal evolution of the slump or to the structures generated during subsequent reactivation and reworking (see Alsop and Marco, 2011). This broad subdivision of slumps does however provide a useful non-generic framework in which to further analyse deformational features, and allows our detailed case study to draw some general conclusions listed below.

- Failure and slumping on very gentle slopes ($<1^\circ$) can be facilitated by increases in pore fluid pressure triggered by seismicity, and loading associated with translation of slump sheets themselves. In addition, exceptional layer cake stratigraphies, as developed on a cm-scale within lacustrine environments, potentially provide numerous easy-slip horizons to facilitate further slump translation.
- The presence of classic Type 1, 2 and 3 re-fold patterns indicates that progressive deformation generated within a single slump event (perhaps lasting just a few minutes) is capable of creating structural relationships that traditionally have been considered representative of separate or punctuated episodes in metamorphic terranes.
- Curvilinear sheath folds created when fold hinges rotate towards the flow direction, and newly classified cylindrical *spiral folds* generated when hinges disarticulate and roll downslope can both be created during slumping. The style of fold that forms reflects initial fold hinge orientation, geometry and amount of deformation.
- Fold hinges and axial planes define clustered and grouped patterns within coherent slump sheets, and become progressively more scattered as slumps evolve into semi-coherent and incoherent masses with increasing deformation accompanied by the breakdown of aragonite-mud laminae. Folds and associated axial planes generated when the slump is relatively coherent thereby provide the best opportunity for palaeoslope analysis.
- Heterogeneous multi layers combined with extreme deformation may generate semi-detached fold trains in which the hinges and short limbs of verging fold pairs are relatively thickened resulting in newly classified *X folds*. Apophyses representing the hinge and short limb of the sheared fold pair can still be used to determine original fold vergence.
- Small-scale parasitic folds frequently developed around larger folds in metamorphic terranes are notably lacking around slump folds. This absence simply reflects the rapid rates of deformation, more limited competency contrasts and lack of an overlying confining layer when slumps are compared to metamorphic terranes.
- An analysis of low angle slope failures associated with recent slumping permits a rigorous testing of established kinematic and geometric models, as recent structures are investigated and interpreted in 3-D with fewer unknown variables.

Acknowledgements

We thank Mr. John Levy, together with the Carnegie Trust and the Royal Society of Edinburgh for travel grants to IA, and the Israel Science Foundation for grant 1539/08 to SM. SM also thanks the Department of

Earth Sciences at Durham University for hosting a visit. Finally we thank Hugo Ortner, an anonymous referee, and Ivo Baron for providing detailed comments that helped clarify this paper.

References

- Aftabi, P., Rostaie, M., Alsop, G.I., Talbot, C.J., 2010. InSAR mapping and modelling of an active Iranian salt extrusion. *Journal of the Geological Society of London* 167, 155–170.
- Agnon, A., Migowski, C., Marco, S., 2006. Intraclast breccia layers in laminated sequences: recorders of paleo-earthquakes. In: Enzel, Y., Agnon, A., Stein, M. (Eds.), *New Frontiers in Dead Sea Paleoenvironmental Research: Geological Society of America Special Publication*, pp. 195–214.
- Allen, J.R.L., 1982. Sedimentary structures, their character and physical basis. *Developments in Sedimentology*, 30. Elsevier, Amsterdam (663 pp.).
- Alsop, G.I., 1992. Progressive deformation and the rotation of contemporary fold axes in the Ballybofey Nappe, north-west Ireland. *Geological Journal* 27, 271–283.
- Alsop, G.I., 1994. Relationships between distributed and localized shear in the tectonic evolution of a Caledonian fold and thrust zone, northwest Ireland. *Geological Magazine* 131, 123–136.
- Alsop, G.I., Carreras, J., 2007. Structural evolution of sheath folds: a case study from Cap de Creus. *Journal of Structural Geology* 29, 1915–1930.
- Alsop, G.I., Holdsworth, R.E., 2007. Flow perturbation folding in shear zones. In: Ries, A.C., Butler, R.W.H., Graham, R.D. (Eds.), *Deformation of the Continental Crust: The Legacy of Mike Coward: Geological Society, London, Special Publications*, 272, pp. 77–103.
- Alsop, G.I., Holdsworth, R.E., 2012. The three dimensional shape and localisation of deformation within multilayer sheath folds. *Journal of Structural Geology* 44, 110–128. <http://dx.doi.org/10.1016/j.jsg.2012.08.015>.
- Alsop, G.I., Marco, S., 2011. Soft-sediment deformation within seismogenic slumps of the Dead Sea Basin. *Journal of Structural Geology* 33, 433–457.
- Alsop, G.I., Marco, S., 2012a. A large-scale radial pattern of seismogenic slumping towards the Dead Sea Basin. *Journal of the Geological Society of London* 169, 99–110. <http://dx.doi.org/10.1144/0016-76492011-032>.
- Alsop, G.I., Marco, S., 2012b. Tsunami and seiche-triggered deformation within offshore sediments. *Sedimentary Geology* 261, 90–107.
- Alsop, G.I., Holdsworth, R.E., McCaffrey, K.J.W., 2007. Scale invariant sheath folds in salt, sediments and shear zones. *Journal of Structural Geology* 29, 1585–1604.
- Alsop, G.I., Cheer, D.A., Strachan, R.A., Krabbendam, M., Kinny, P.D., Holdsworth, R.E., Leslie, A.G., 2010. Progressive fold and fabric evolution associated with regional strain gradients: a case study from across a Scandian ductile thrust nappe, Scottish Caledonides. In: Law, R.D., Butler, R.W.H., Holdsworth, R.E., Krabbendam, M., Strachan, R.A. (Eds.), *Continental Tectonics and Mountain Building: The Legacy of Peach and Horne: Geological Society, London, Special Publications*, 335, pp. 253–272.
- Bartov, Y., Steinitz, G., Eyal, M., Eyal, Y., 1980. Sinistral movement along the Gulf of Aqaba – its age and relation to the opening of the Red Sea. *Nature* 285, 220–221.
- Begin, Z.B., Ehrlich, A., Nathan, Y., 1974. Lake Lisan, the Pleistocene precursor of the Dead Sea. *Geological Survey of Israel Bulletin* 63, 30.
- Begin, Z.B., Steinberg, D.M., Ichinose, G.A., Marco, S., 2005. A 40,000 years unchanging of the seismic regime in the Dead Sea rift. *Geology* 33, 257–260.
- Bradley, D., Hanson, L., 1998. Paleoslope analysis of slump folds in the Devonian flysch of Main. *Journal of Geology* 106, 305–318.
- Bull, S., Cartwright, J., Huuse, M., 2009. A review of kinematic indicators from mass-transport complexes using 3D seismic data. *Marine and Petroleum Geology* 26, 1132–1151.
- Butler, R.W.H., Paton, D.A., 2010. Evaluating lateral compaction in deepwater fold and thrust belts: how much are we missing from nature's sandbox? *GSA Today* 20, 4–10. *Chambers Dictionary*, 1993. Chambers Harrap Publishers Ltd, Edinburgh.
- Collins English Dictionary & Thesaurus, 2000. 2nd ed. HarperCollins Publishers, Glasgow.
- Collinson, J., 1994. Sedimentary deformational structures. In: Maltman, A.J. (Ed.), *The Geological Deformation of Sediments*. Chapman and Hall, London, pp. 95–125.
- Corbett, K.D., 1973. Open-cast slump sheets and their relationship to sandstone beds in an Upper Cambrian flysch sequence, Tasmania. *Journal of Sedimentary Petrology* 43, 147–159.
- Dasgupta, P., 2008. Experimental decipherment of the soft-sediment deformation observed in the upper part of the Talchir Formation (Lower Permian), Jharia Basin, India. *Sedimentary Geology* 205, 100–110.
- Debacker, T.N., Sintubin, M., Verniers, J., 2001. Large-scale slumping deduced from structural and sedimentary features in the Lower Palaeozoic Anglo-Brabant fold belt, Belgium. *Journal of the Geological Society of London* 158, 341–352.
- Debacker, T.N., van Noorden, M., Sintubin, M., 2006. Distinguishing syn-cleavage folds from pre-cleavage folds to which cleavage is virtually axial planar: examples from the Cambrian core of the Lower Palaeozoic Anglo-Brabant Deformation Belt (Belgium). *Journal of Structural Geology* 28, 1123–1138.
- Debacker, T.N., Dumon, M., Matthys, A., 2009. Interpreting fold and fault geometries from within the lateral to oblique parts of slumps: a case study from the Anglo-Brabant Deformation Belt (Belgium). *Journal of Structural Geology* 31, 1525–1539.
- Druguet, E., Alsop, G.I., Carreras, J., 2009. Coeval brittle and ductile structures associated with extreme deformation partitioning in a multilayer sequence. *Journal of Structural Geology* 31, 498–511.
- Dzulynski, S., Walton, E.K., 1965. *Sedimentary Features of Flysch and Greywackes*. Elsevier, Amsterdam (274 pp.).
- Elliot, C.G., Williams, P.F., 1988. Sediment slump structures: a review of diagnostic criteria and application to an example from Newfoundland. *Journal of Structural Geology* 10, 171–182.

- Escher, A., Watterson, J., 1974. Stretching fabrics, folds and crustal shortening. *Tectonophysics* 22, 223–231.
- Farrell, S.G., 1984. A dislocation model applied to slump structures, Ainsa Basin, South Central Pyrenees. *Journal of Structural Geology* 6, 727–736.
- Farrell, S.G., Eaton, S., 1987. Slump strain in the Tertiary of Cyprus and the Spanish Pyrenees. Definition of palaeoslopes and models of soft sediment deformation. In: Jones, M.F., Preston, R.M.F. (Eds.), *Deformation of Sediments and Sedimentary Rocks: Special Publication of the Geological Society of London*, 29, pp. 181–196.
- Farrell, S.G., Eaton, S., 1988. Foliations developed during slump deformation of Miocene marine sediments, Cyprus. *Journal of Structural Geology* 10, 567–576.
- Field, M.E., Gardner, J.V., Jennings, A.E., Edwards, B.D., 1982. Earthquake-induced sediment failures on a 0.25° slope, Klamath River delta, California. *Geology* 10, 542–546.
- Flinn, D., 1962. On folding during three-dimensional progressive deformation. *Quarterly Journal of the Geological Society of London* 118, 385–433.
- Fossen, H., 2010. *Structural Geology*. Cambridge University Press, Cambridge, UK (463 pp.).
- Fossen, H., Rykkeldid, E., 1990. Shear zone structures in the Øygarden area, West Norway. *Tectonophysics* 174, 385–397.
- Frehner, M., Schmalholtz, S.M., 2006. Numerical simulations of parasitic folding in multilayers. *Journal of Structural Geology* 28, 1647–1657.
- García-Tortosa, F.J., Alfaro, P., Gilbert, L., Scott, G., 2011. Seismically induced slump on an extremely gentle slope (<1°) of the Pleistocene Tecopa paleolake (California). *Geology* 39, 1055–1058.
- Gardner, J.V., Prior, D.B., Field, M.E., 1999. Humboldt slide — a large shear dominated retrogressive slope failure. *Marine Geology* 154, 323–338.
- Garfunkel, Z., 1981. Internal structure of the Dead Sea leaky transform (rift) in relation to plate kinematics. *Tectonophysics* 80, 81–108.
- Garfunkel, Z., Ben-Avraham, Z., 1996. The structure of the Dead Sea Basin. *Tectonophysics* 26, 155–176.
- Gilbert, L., Sanz de Galdeano, C., Alfaro, P., Scott, G., Lopez Garrido, A.C., 2005. Seismic-induced slump in Early Pleistocene deltaic deposits of the Baza Basin (SE Spain). *Sedimentary Geology* 179, 279–294.
- Ginzburg, A., Ben-Avraham, Z., 1997. A seismic reflection study of the north basin of the dead sea, Israel. *Geophysical Research Letters* 24 (16), 2063–2066.
- Haase-Schramm, A., Goldstein, S.L., Stein, M., 2004. U-Th dating of Lake Lisan aragonite (late Pleistocene Dead Sea) and implications for glacial East Mediterranean climate change. *Geochimica et Cosmochimica Acta* 68, 985–1005.
- Hansen, E., 1971. *Strain Facies*. Springer-Verlag, Berlin (207 pp.).
- Heifetz, E., Agnon, A., Marco, S., 2005. Soft sediment deformation by Kelvin Helmholtz instability: a case from Dead Sea earthquakes. *Earth and Planetary Science Letters* 236, 497–504.
- Holdsworth, R.E., 1988. The stereographic analysis of facing. *Journal of Structural Geology* 10, 219–223.
- Hudleston, P.J., Treagus, S.H., 2010. Information from folds: a review. *Journal of Structural Geology* 32, 2042–2071.
- Hurst, A., Scott, A., Vigorito, M., 2011. Physical characteristics of sand injectites. *Earth-Science Reviews* 106, 215–246.
- Jackson, C.A.-L., 2011. Three-dimensional seismic analysis of megaclast deformation within a mass transport deposit: implications for debris flow kinematics. *Geology* 39, 203–206.
- Jiang, D.Z., Williams, P.F., 1999. When do drag folds not develop into sheath folds in shear zones? *Journal of Structural Geology* 21, 577–583.
- Jones, O.T., 1939. The geology of the Colwyn bay district: a study of submarine slumping during the Salopian period. *Quarterly Journal of the Geological Society of London* 380, 335–382.
- Kagan, E., Stein, M., Agnon, A., Neumann, F., 2011. Intrabasin paleoearthquake and quiescence correlation of the Late Holocene Dead Sea. *Journal of Geophysical Research* 116 (B4), B04311.
- Ken-Tor, R., Agnon, A., Enzel, Y., Marco, S., Negendank, J.F.W., Stein, M., 2001. High-resolution geological record of historic earthquakes in the Dead Sea basin. *Journal of Geophysical Research* 106, 2221–2234.
- Knipe, R.J., 1986. Deformation mechanism path diagrams for sediments undergoing lithification. *Memoir of the Geological Society of America* 166, 151–160.
- Lajoie, J., 1972. Slump fold axis orientations: an indication of palaeoslope? *Journal of Sedimentary Petrology* 42, 584–586.
- Lee, H.J., Locat, J., Desgagnés, P., Parsons, J.D., McAdoo, B.G., Orange, D.L., Puig, P., Wong, F.L., Dartnell, P., Boulanger, E., 2007. Submarine mass movements on continental margins. In: Nittrouer, C.A., Austin, J.A., Field, M.E., Kravitz, J.H., Syvitski, J.P.M., Wiberg, P.L. (Eds.), *Continental Margin Sedimentation: From Sediment Transport to Sequence Stratigraphy*. Special Publication of the International Association of Sedimentologists, 37. Blackwell Publishing, pp. 213–274.
- Leseman, J.-E., Alsop, G.I., Piotrowski, J.A., 2010. Incremental subglacial meltwater sediment deposition and deformation associated with repeated ice-bed decoupling: a case study from the Island of Funen, Denmark. *Quaternary Science Reviews* 29, 3212–3229.
- Levi, T., Weinberger, R., Aifa, T., Eyal, Y., Marco, S., 2006. Injection mechanism of clay-rich sediments into dikes during earthquakes. *Geochemistry, Geophysics, Geosystems* 7 (12), Q12009. <http://dx.doi.org/10.1029/2006GC001410>.
- Lewis, K.B., 1971. Slumping on a continental slope inclined at 1–4°. *Sedimentology* 16, 97–110.
- Locat, J., Lee, H.J., 2002. Submarine landslides: advances and challenges. *Canadian Geotechnical Journal* 39, 193–212.
- Maltman, A., 1984. On the term soft-sediment deformation. *Journal of Structural Geology* 6, 589–592.
- Maltman, A., 1994a. *The Geological Deformation of Sediments*. Chapman & Hall, London (362 pp.).
- Maltman, A., 1994b. Introduction and overview. In: Maltman, A. (Ed.), *The Geological Deformation of Sediments*. Chapman & Hall, London, pp. 1–35.
- Maltman, A., 1994c. Deformation structures preserved in rocks. In: Maltman, A. (Ed.), *The Geological Deformation of Sediments*. Chapman & Hall, London, pp. 261–307.
- Marco, S., Agnon, A., 1995. Prehistoric earthquake deformations near Masada, Dead Sea graben. *Geology* 23, 695–698.
- Marco, S., Agnon, A., 2005. High-resolution stratigraphy reveals repeated earthquake faulting in the Masada Fault Zone, Dead Sea Transform. *Tectonophysics* 408 (1–4), 101–112.
- Marco, S., Stein, M., Agnon, A., Ron, H., 1996. Long term earthquake clustering: a 50,000 year paleoseismic record in the Dead Sea Graben. *Journal of Geophysical Research* 101, 6179–6192.
- Marco, S., Weinberger, R., Agnon, A., 2002. Radial clastic dykes formed by a salt diapir in the Dead Sea Rift, Israel. *Terra Nova* 14, 288–294.
- Marco, S., Hartal, M., Hazan, N., Lev, L., Stein, M., 2003. Archaeology, history, and geology of the A.D. 749 earthquake, Dead Sea Transform. *Geology* 31, 665–668.
- Martinsen, O.J., 1989. Styles of soft-sediment deformation on a Namurian delta slope, Western Irish Namurian Basin, Ireland. In: Whateley, M.K.G., Pickering, K.T. (Eds.), *Deltas: Sites and Traps for Fossil Fuels*. Geological Society of London Special Publication, 41. Geological Society London, London, pp. 167–177.
- Martinsen, O.J., 1994. Mass movements. In: Maltman, A. (Ed.), *The Geological Deformation of Sediments*. Chapman & Hall, London, pp. 127–165.
- Martinsen, O.J., Bakken, B., 1990. Extensional and compressional zones in slumps and slides in the Namurian of County Claire, Eire. *Journal of the Geological Society of London* 147, 153–164.
- Mason, D., Habitz, C., Wynn, R., Pederson, G., Lovholt, F., 2006. Submarine landslides: processes, triggers and hazard protection. *Philosophical Transactions of the Royal Society* 364, 2009–2039.
- McClelland, H.L.O., Woodcock, N.H., Gladstone, C., 2011. Eye and sheath folds in turbidite convolute lamination: Aberystwyth Grits Group, Wales. *Journal of Structural Geology* 33, 1140–1147.
- Migowski, C., Agnon, A., Bookman, R., Negendank, J.F.W., Stein, M., 2004. Recurrence pattern of Holocene earthquakes along the Dead Sea Transform revealed by varve-counting and radiocarbon dating of lacustrine sediments. *Earth and Planetary Science Letters* 222, 301–314.
- Moernaut, J., De Batist, M., 2011. Frontal emplacement and mobility of sublacustrine landslides: results from morphometric and seismostratigraphic analysis. *Marine Geology* 285, 29–45.
- Ortner, H., 2007. Styles of soft-sediment deformation on top of a growing fold system in the Gosau Group at Mutteköpf, Northern Calcareous Alps, Austria: slumping versus tectonic deformation. *Sedimentary Geology* 196, 99–118.
- Owen, G., 1996. Experimental soft-sediment deformation: structures formed by the liquefaction of unconsolidated sands and some ancient examples. *Sedimentology* 43, 279–293.
- Passchier, C.W., Trouw, R.A.J., 2005. *Microtectonics*, 2nd edition. Springer (366 pp.).
- Pickering, K.T., 1987. Wet-sediment deformation in the Upper Ordovician Point Leamington Formation: an active thrust imbricate system during sedimentation, Notre Dame Bay, north-central Newfoundland. In: Jones, M.E., Preston, R.M.F. (Eds.), *Deformation of Sediments and Sedimentary Rocks: Geological Society Special Publication*, 29, pp. 213–239.
- Pisarska-Jamroz, M., Weckwerth, P., 2012. Soft-sediment deformation structures in a Pleistocene glaciolacustrine delta and their implications for the recognition of subenvironments in delta deposits. *Sedimentology*. <http://dx.doi.org/10.1111/j.1365-3091.2012.01354.x>.
- Porat, N., Levi, T., Weinberger, R., 2007. Possible resetting of quartz OSL signals during earthquakes — evidence from Late Pleistocene injection dikes, Dead Sea Basin, Israel. *Quaternary Geochronology* 2, 272–277.
- Ramsay, J.G., 1967. *Folding and Fracturing of Rocks*. McGraw Hill, New York (568 pp.).
- Ramsay, J.G., Huber, M.I., 1987. *The techniques of modern structural geology. Folds and Fractures*, volume 2. Academic Press.
- Sengupta, S., Ghosh, S.K., Deb, S.K., Khan, D., 2005. Opening and closing of folds in superposed deformations. *Journal of Structural Geology* 27, 1282–1299.
- Shackleton, R.M., 1958. Downward-facing structures of the Highland Border. *Quarterly Journal of the Geological Society of London* 113, 361–392.
- Smith, J.V., 2000. Flow pattern within a Permian submarine slump recorded by oblique folds and deformed fossils, Ulladulla, south-eastern Australia. *Sedimentology* 47, 357–366.
- Strachan, L.J., 2002. Slump-initiated and controlled syndepositional sandstone remobilization; an example from the Namurian of County Clare, Ireland. *Sedimentology* 49, 25–41.
- Strachan, L.J., 2008. Flow transformations in slumps: a case study from the Waitemata Basin, New Zealand. *Sedimentology* 55, 1311–1332.
- Strachan, L.J., Alsop, G.I., 2006. Slump folds as estimators of palaeoslope: a case study from the Fisherstreet Slump of County Clare, Ireland. *Basin Research* 18, 451–470.
- Treagus, S.H., Fletcher, R.C., 2009. Controls of folding on different scales in multilayered rocks. *Journal of Structural Geology* 31, 1340–1349.
- Treagus, J.E., Treagus, S.H., 1981. Folds and the strain ellipsoid: a general model. *Journal of Structural Geology* 3, 1–17.
- Turner, F.J., Weiss, L.E., 1963. *Structural Analysis of Metamorphic Tectonites*. McGraw-Hill, New York.
- Twiss, R.J., Moores, E.M., 1992. *Structural Geology*. W.H. Freeman and Company, New York (532 pp.).
- Van Loon, A.J., Han, Z., Han, Y., 2012. Slide origin of breccia lenses in the Cambrian of the North China Platform: new insight into mass transport in an epeiric sea. *Geology* 18, 223–235.

- Waldron, J.W.F., Gagnon, J.-F., 2011. Recognizing soft-sediment structures in deformed rocks of orogens. *Journal of Structural Geology* 33, 271–279.
- Wells, J.T., Prior, D.B., Coleman, J.M., 1980. Flowslides in muds on extremely low angle tidal flats, northeastern South America. *Geology* 8, 272–275.
- Wetzler, N., Marco, S., Heifetz, E., 2009. Quantitative analysis of seismogenic shear-induced turbulence in lake sediments. *Geology* 38, 303–306.
- Woodcock, N.H., 1976a. Ludlow Series slumps and turbidites and the form of the Montgomery Trough, Powys, Wales. *Proceedings of the Geologists Association* 87, 169–182.
- Woodcock, N.H., 1976b. Structural style in slump sheets: Ludlow Series, Powys, Wales. *Journal of the Geological Society of London* 132, 399–415.
- Woodcock, N.H., 1979. The use of slump structures as palaeoslope orientation estimators. *Sedimentology* 26, 83–99.